

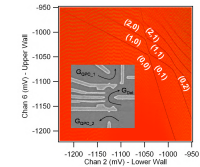
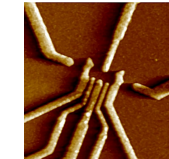
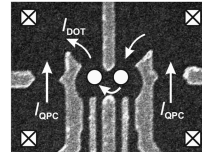
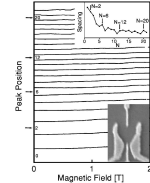
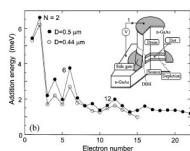
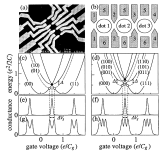
# Spin Qubits in Semiconducting Nanostructures II

Daniel Loss  
Department of Physics  
University of Basel

\$\$: Swiss NSF, Nano Basel, Quantum ETH/Basel, EU

# Spin qubits in GaAs quantum dots

Kloeffel & DL, Annu. Rev. Condens. Matter Phys. 4, 51 (2013)



Westervelt  
Gossard 1995

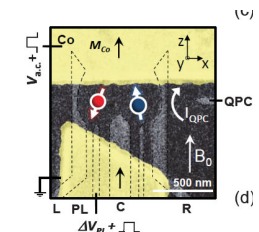
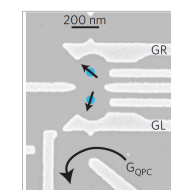
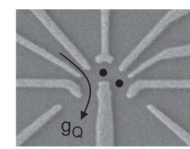
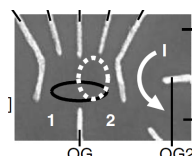
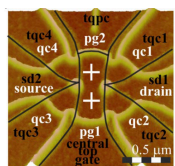
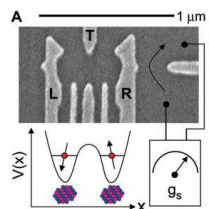
Kouwenhoven  
Tarucha 1996

Sachrajda  
2000

Kouwenhoven  
Tarucha 2003-13

Vandersypen,  
Koppens, 2003

Marcus 2004



Petta, Marcus,  
Yacoby 2005

Ensslin, Ihn  
2006

Zumbuhl,  
Kastner  
2008

Petta 2010

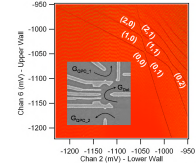
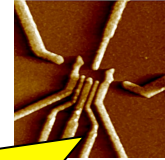
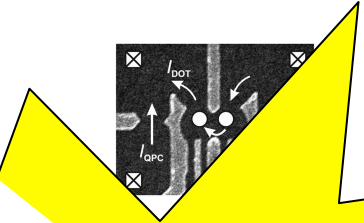
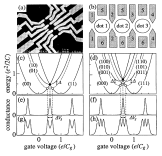
Bluhm, Dial,  
Yacoby 2010-13  
 $T_2 \sim 300 \mu\text{s}$

Brunner,  
Pioro-Ladriere,  
Tarucha 2011

... and many more ...

# Spin qubits in GaAs quantum dots

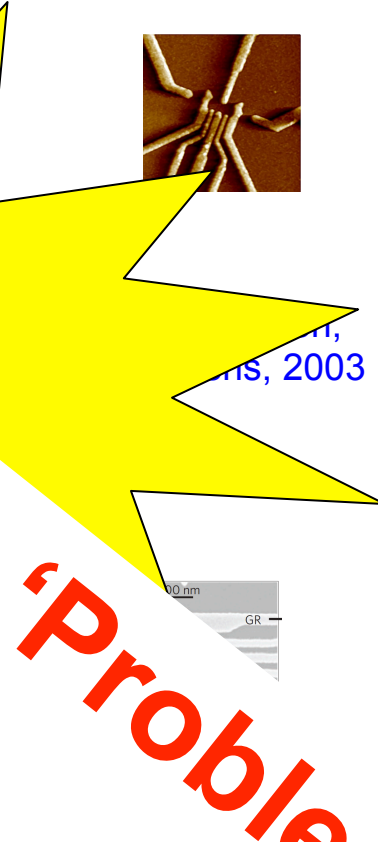
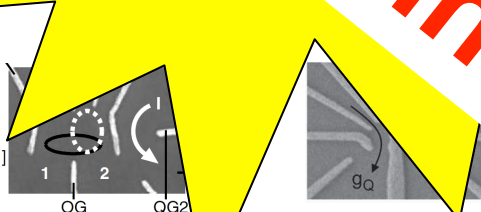
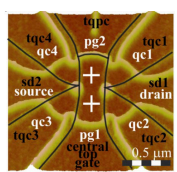
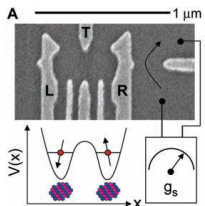
& DL, Annu. Rev. Condens. Matter Phys. 4, 51 (2013)



Westervelt  
Gossard 1995

Kouwenhoven,  
Tarucha, Lounsbury,  
Hanson, 2003

Marcus 2004



Petta, Marcus,  
Yacoby 2005

Ensslin, Ihn  
2006

Zumbuhl,  
Kastner  
2008

Petta 2010

Bluhm, Dial,  
Yacoby 2010 - ,  
 $T_2 \sim 300 \mu\text{s}$

Forster,  
Fries, 2011

... and many more ...

**GaAs: Nuclear Spin 'Problem'?**

## Strategies:

1. Use GaAs (still ‘best’ material for electrical control) and deal with nuclear spins  
→ echo techniques and/or dynamical narrowing

Bluhm & Yacoby et al., Nat. Phys. 7, 109 (2011)  
Kuemmeth & Marcus et al., Nat. Nano 12, 16 (2017):  $T_2 \sim 1\text{ms}$
2. Avoid nuclear spin problem: use holes and/or other materials such as isotopically purified C, Si, Ge,...

# Electron vs. Hole Spin Qubits

# Band Diagram Near $\Gamma$ Point ( $k = 0$ )

Typical bulk spectrum  
of a semiconductor:

*Higher bands*



**Conduction band**  
s-type Bloch functions



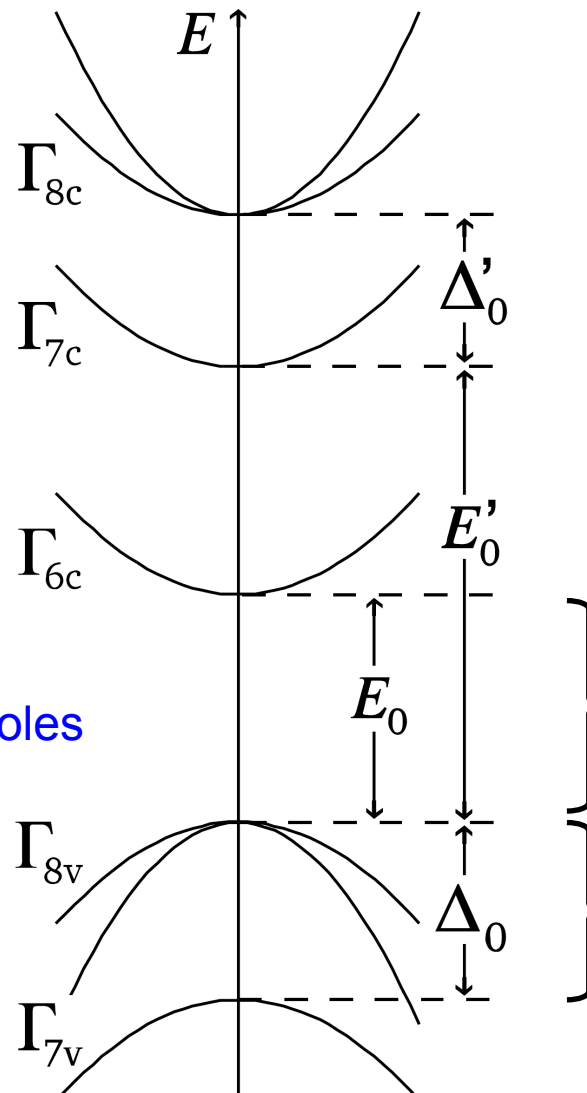
Spin 3/2, Heavy holes and light holes



**Valence band**  
p-type Bloch functions



*Split-Off Band*



**GaAs:**

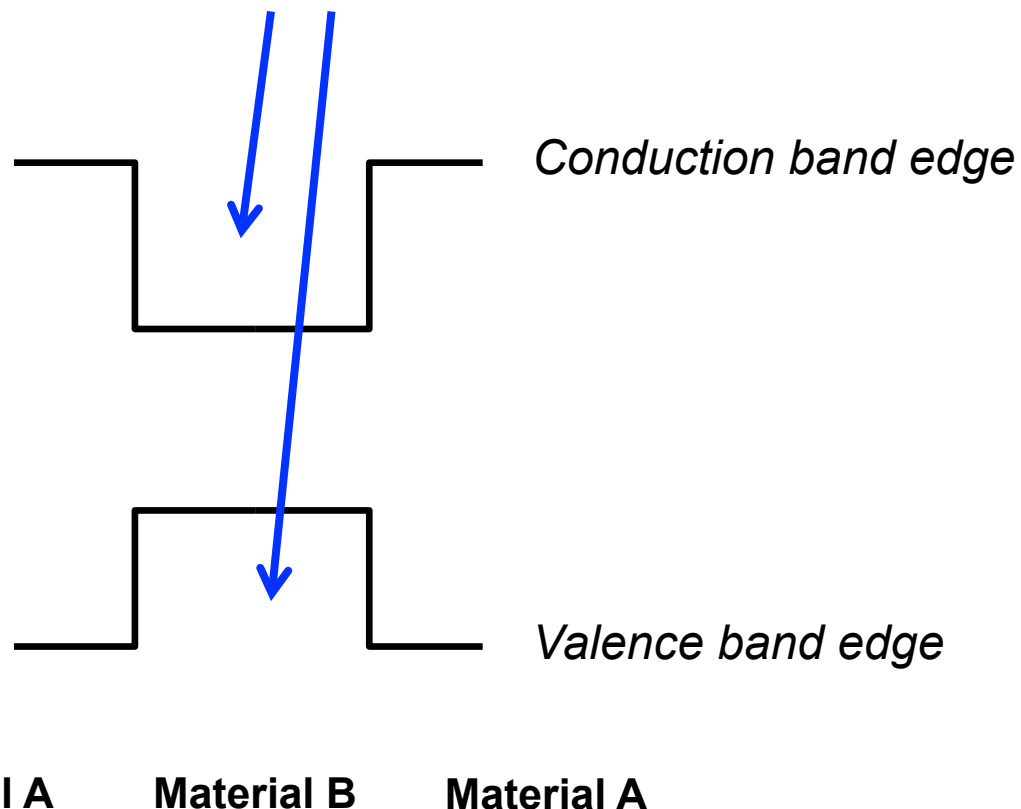
**band gap**  
1.5 eV

0.3 eV

# Quantum Well: Examples

Type I

Both electrons and holes can  
be trapped in material B



Example:

GaAs

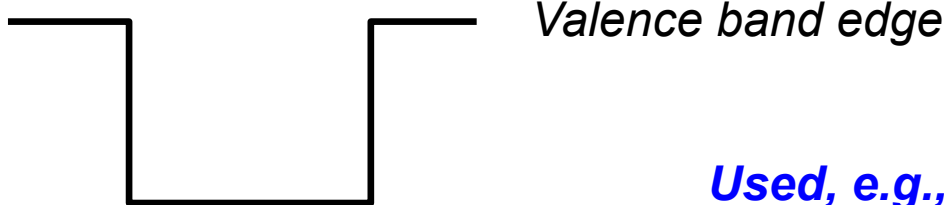
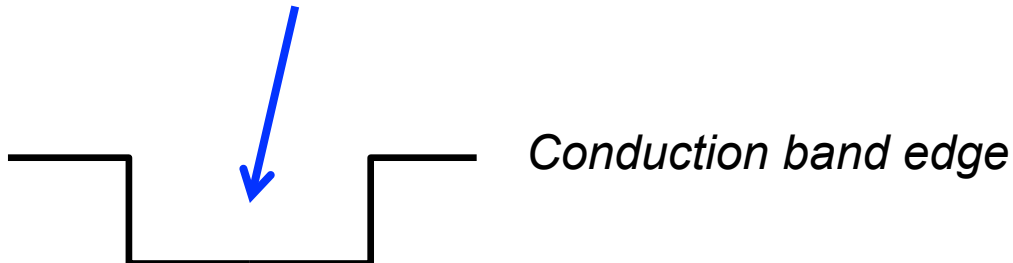
InGaAs

GaAs

# Quantum Well: Examples

Type II  
*for electrons*

Only electrons can be  
trapped in material B



Used, e.g., in Si-SiGe  
heterostructures to  
form a 2DEG in Si

Material A      Material B      Material A

Example:

Ge

Si

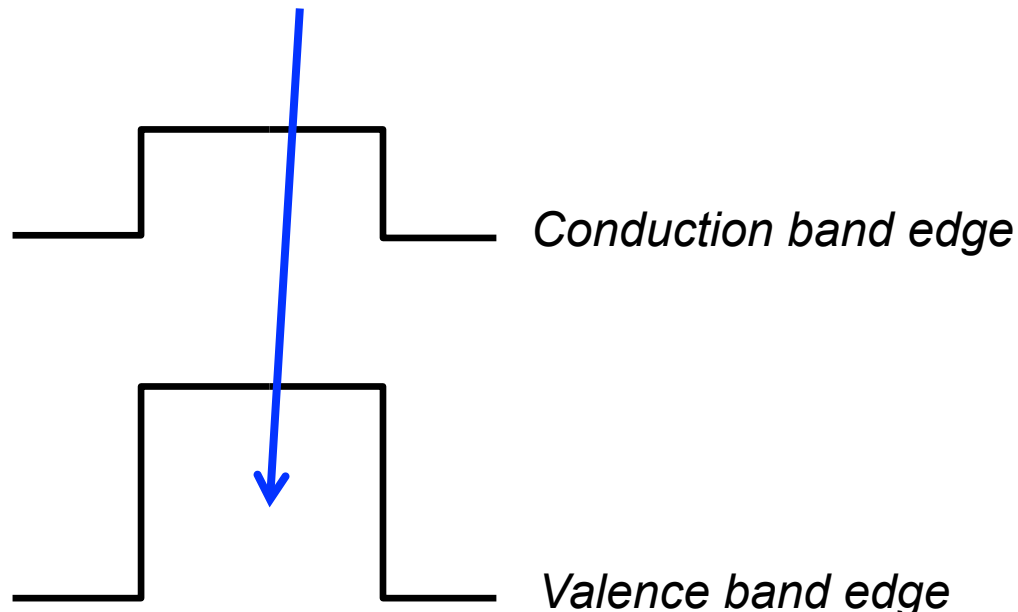
Ge

# Quantum Well: Examples

Type II  
*for holes*

*Used, e.g., in Ge-SiGe  
heterostructures to  
form a 2DHG in Ge*

Only holes can be  
trapped in material B



Material A      Material B      Material A

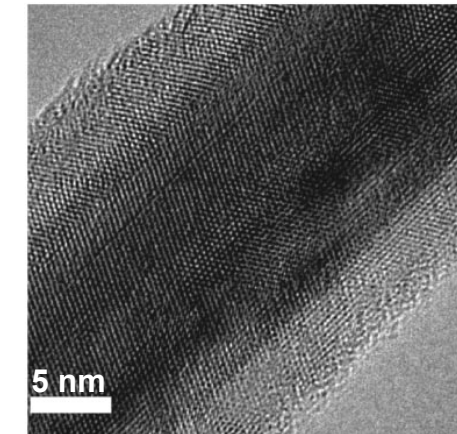
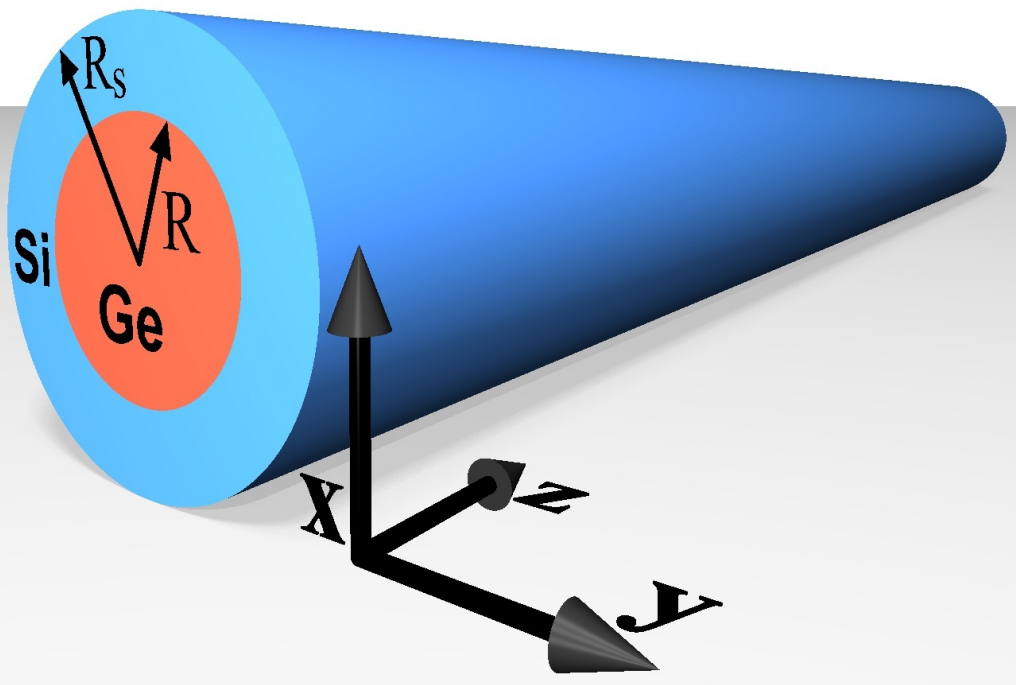
Example:

Si

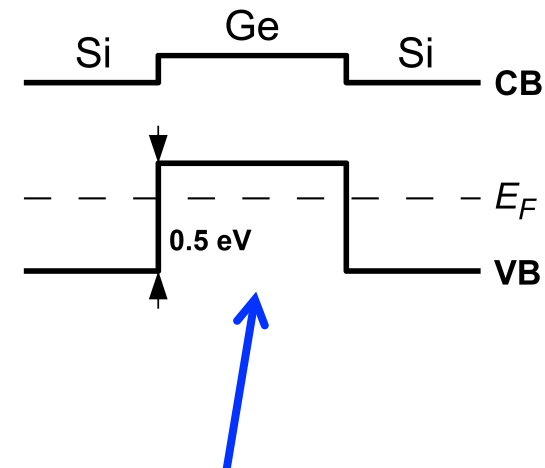
Ge

Si

# Ge/Si Core/Shell Nanowires



HR-TEM, Lieber (2005)



Lauhon *et al.*, Nature (2002)  
Lu *et al.*, PNAS USA (2005)  
Kloeffel, Trif, and Loss, PRB (2011)  
Hu *et al.*, Nature Nano (2012)  
...  
...

**Strongly confined holes  
inside the Ge core**

# Hole Spin Qubits in GaAs and InAs

PRL 95, 076805 (2005)

PHYSICAL REVIEW LETTERS

week ending  
12 AUGUST 2005

## Spin Relaxation and Decoherence of Holes in Quantum Dots

Denis V. Bulaev and Daniel Loss

*Department of Physics and Astronomy, University of Basel, Klingelbergstrasse 82, CH-4056 Basel, Switzerland*

(Received 8 March 2005; published 11 August 2005)

We investigate heavy-hole spin relaxation and decoherence in quantum dots in perpendicular magnetic fields. We show that at low temperatures the spin decoherence time is 2 times longer than the spin relaxation time. We find that the spin relaxation time for heavy holes can be comparable to or even longer than that for electrons in strongly two-dimensional quantum dots. We discuss the difference in the magnetic-field dependence of the spin relaxation rate due to Rashba or Dresselhaus spin-orbit coupling for systems with positive (i.e., GaAs quantum dots) or negative (i.e., InAs quantum dots)  $g$  factor.

$$H_{\text{so}}^{\text{HH}} = i\alpha(\sigma_+ P_-^3 - \sigma_- P_+^3) \quad \text{Rashba SOI for HH}$$
$$- \beta(\sigma_+ P_- P_+ P_- + \sigma_- P_+ P_- P_+) \quad \text{Dresselhaus SOI for HH}$$

[EDSR for HHs in III-V materials: Bulaev and DL, PRL 98, 097202 \(2007\)](#)  
ultrafast Rabi oscillations

# Observation of extremely slow hole spin relaxation in self-assembled quantum dots

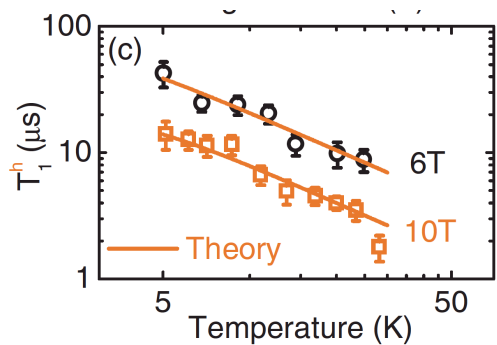
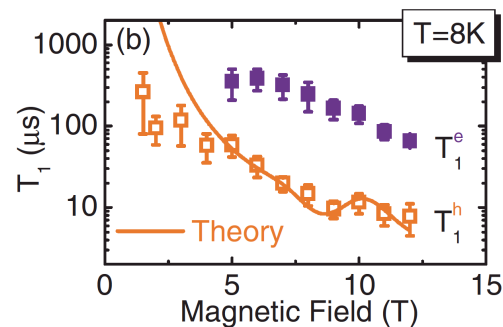
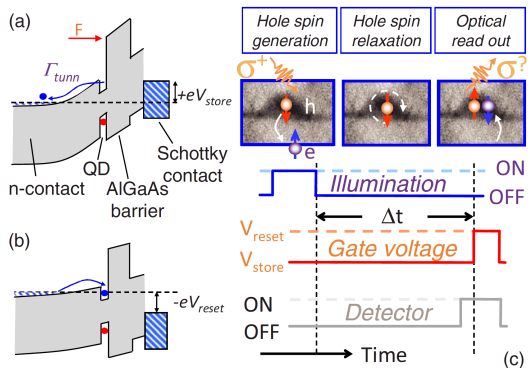
D. Heiss, S. Schaeck, H. Huebl, M. Bichler, G. Abstreiter, and J. J. Finley\*

Walter Schottky Institut, Technische Universität München, Am Coulombwall 3, D-85748 Garching, Germany

D. V. Bulaev and Daniel Loss

Department of Physics and Astronomy, University of Basel, Klingelbergstrasse 82, CH-4056 Basel, Switzerland

(Received 24 October 2007; published 21 December 2007)



# Observation of extremely slow hole spin relaxation in self-assembled quantum dots

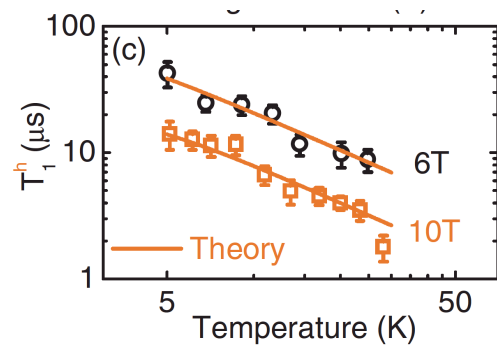
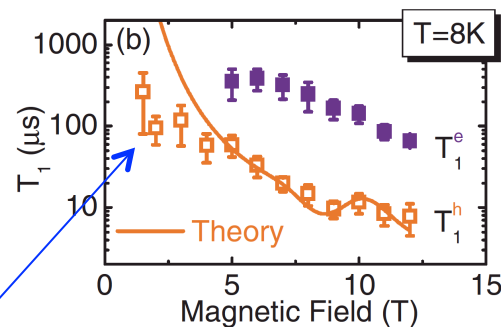
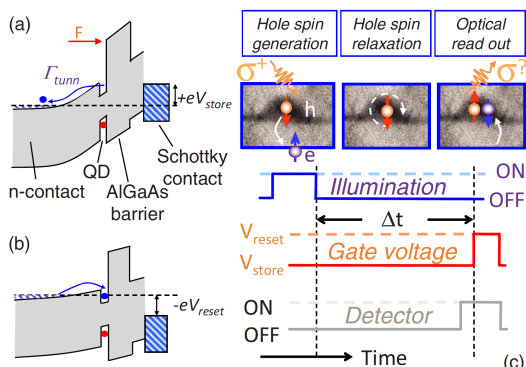
D. Heiss, S. Schaeck, H. Huebl, M. Bichler, G. Abstreiter, and J. J. Finley\*

Walter Schottky Institut, Technische Universität München, Am Coulombwall 3, D-85748 Garching, Germany

D. V. Bulaev and Daniel Loss

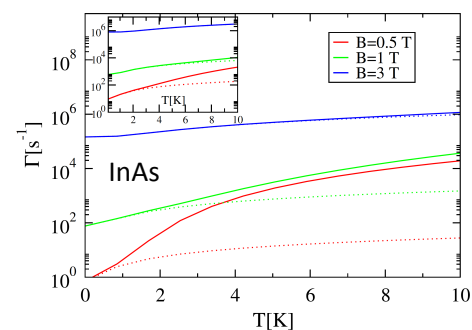
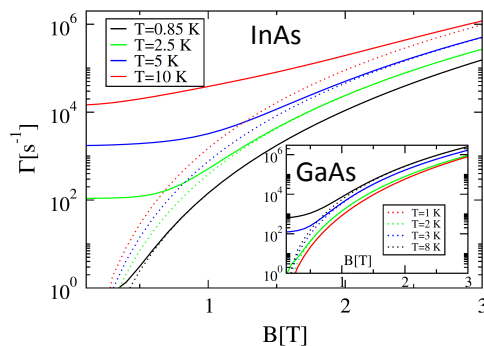
Department of Physics and Astronomy, University of Basel, Klingelbergstrasse 82, CH-4056 Basel, Switzerland

(Received 24 October 2007; published 21 December 2007)



2-Phonon processes  
lead to saturation

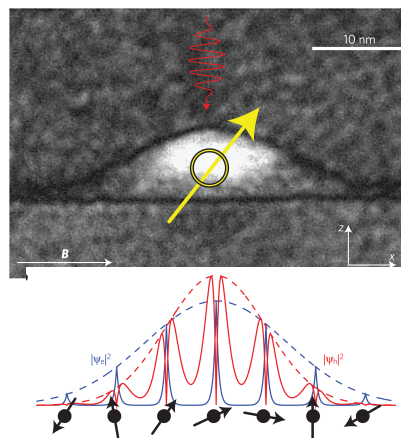
M. Trif, P. Simon, and DL,  
PRL 103, 106601 (2009)



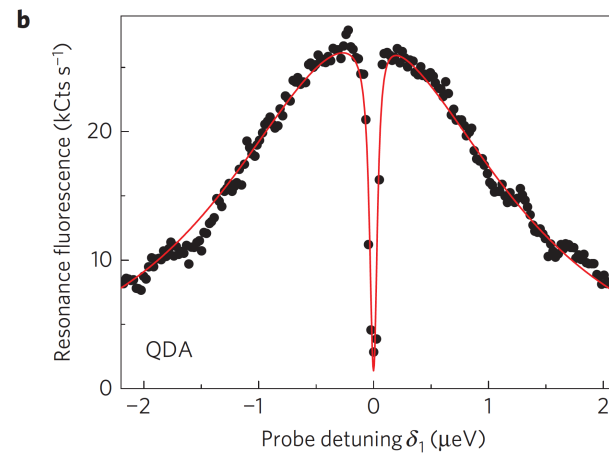
Nature Mat., 2016

# Decoupling a hole spin qubit from the nuclear spins

Jonathan H. Prechtel<sup>1</sup>, Andreas V. Kuhlmann<sup>1</sup>, Julien Houel<sup>1,2</sup>, Arne Ludwig<sup>3</sup>, Sascha R. Valentin<sup>3</sup>, Andreas D. Wieck<sup>3</sup> and Richard J. Warburton<sup>1\*</sup>



InGaAs  
self-assembled dots



Hyperfine interaction  
of holes is nearly Ising  
(transverse < 1%)

$$H = (b_{\perp} + h_z)s_z + b_{\parallel}s_x$$

**b**,  $\Gamma_r = 0.68 \mu\text{eV}$ ,  $T_2 > 1 \mu\text{s}$ ,  $T_1 \gg T_2$ .

# A CMOS silicon hole spin qubit

Maurand et al., Nat. Comm. 7, 13575 (2016)

'quantumize' integrated bits:

→ heavy hole spin in p-doped  
Si-on-Insulator nanowire

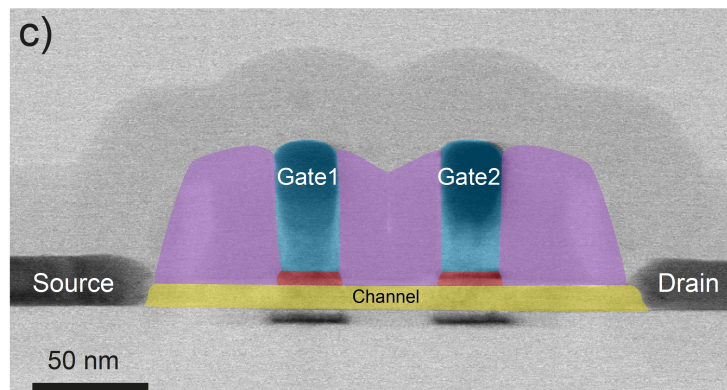
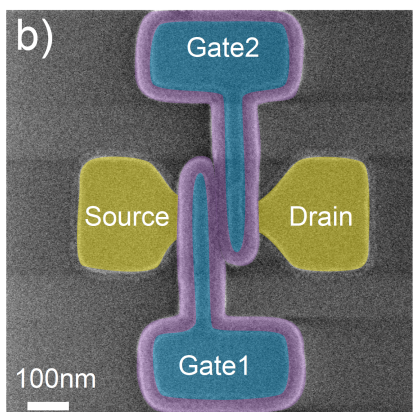
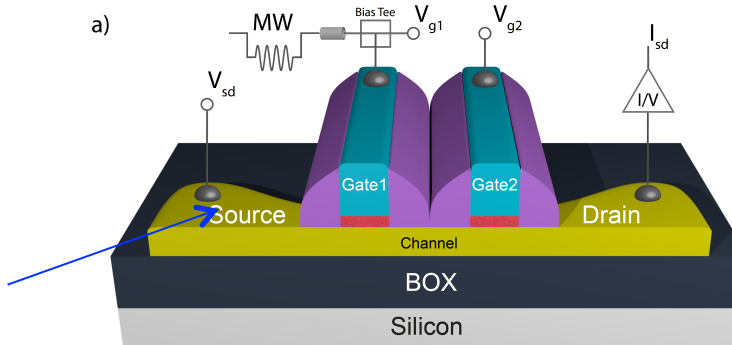


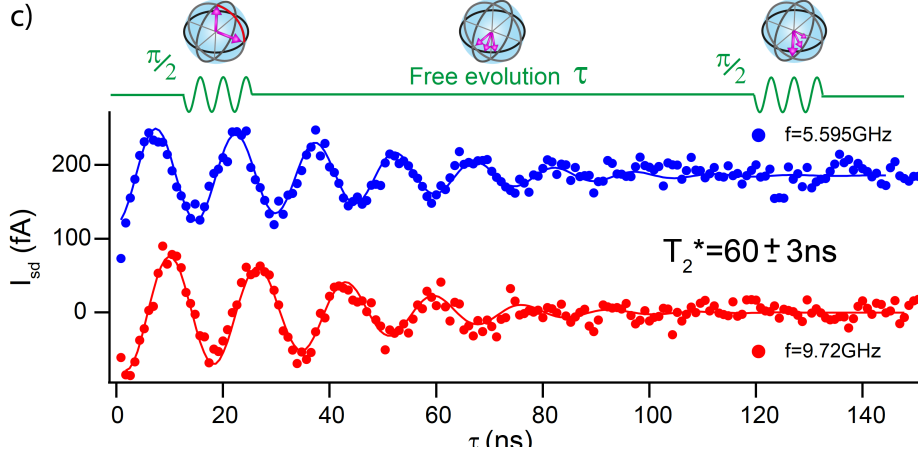
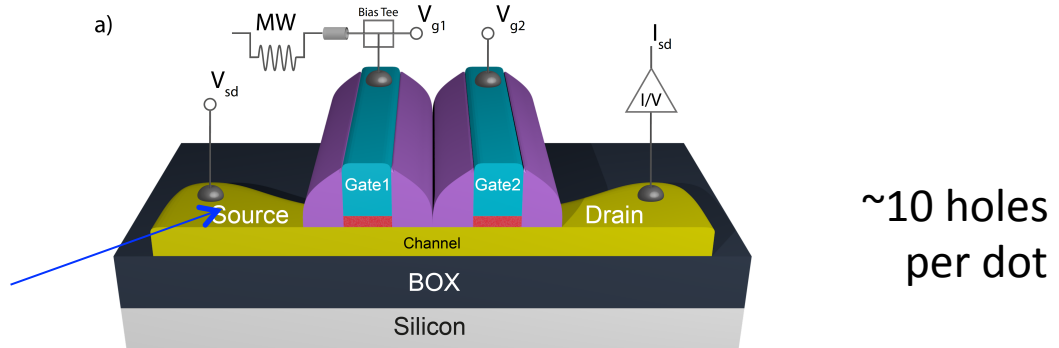
FIG. 1. CMOS qubit device. a, Simplified 3-dimensional schematic of a SOI nanowire field-effect transistor with two gates Gate 1 and Gate 2. Using a bias-T, Gate 1 is connected to a low-pass-filtered line, used to apply a static gate voltage  $V_{g1}$ , and to a 20-GHz bandwidth line, used to apply the high-frequency modulation necessary for qubit initialization, manipulation and readout. b, Colorized device top view obtained by scanning electron microscopy just after the fabrication of gates and spacers. c, Colorized transmission-electron-microscopy image of the device along a longitudinal cross-sectional plane.

# CMOS silicon **hole** spin qubit: Fast EDSR

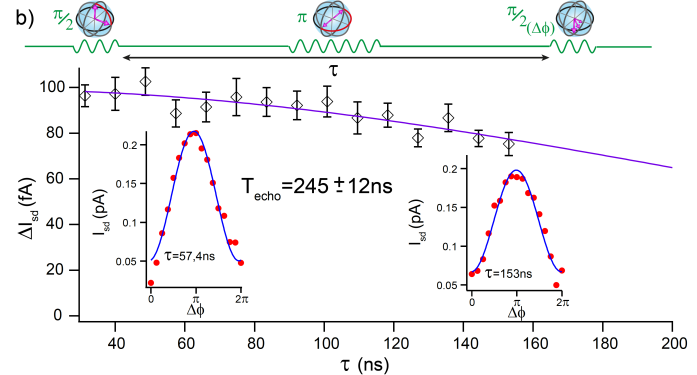
Maurand et al., Nat. Comm. 7, 13575 (2016)

'quantumize' integrated bits:

→ heavy hole spin in p-doped  
Si-on-Insulator nanowire



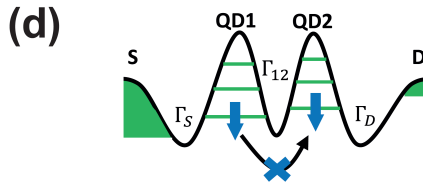
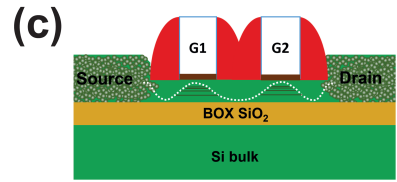
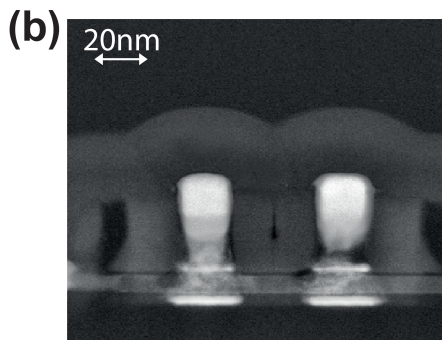
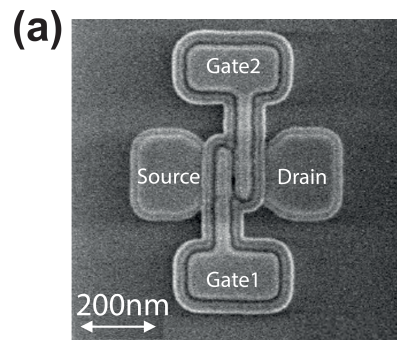
Fast Rabi oscillations ~85 MHz  
and Ramsey fringe via EDSR of holes



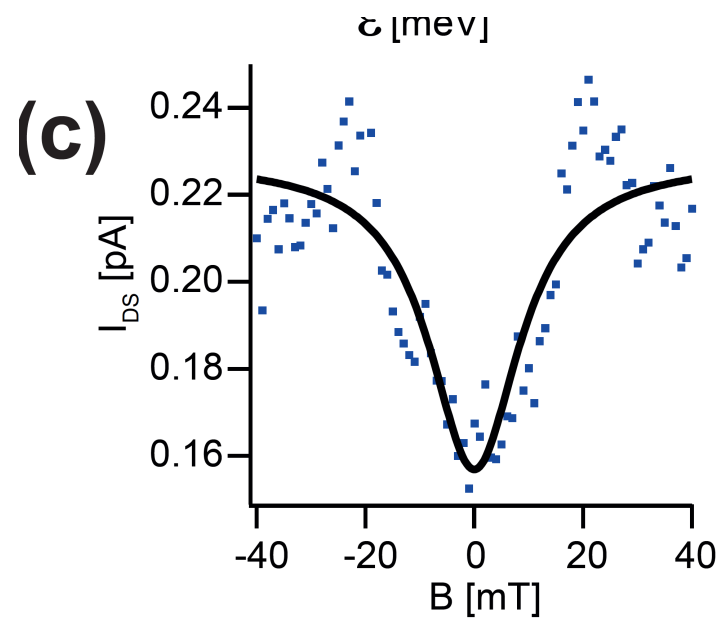
Two-axis qubit control and  
spin coherence times.

# CMOS double dot and PSB

Sanquer & De Franceschi group, Bohuslavskyi et al., arXiv:1607.00287



Pauli spin blockade due to  
spin orbit interaction



# Next Step: Spin Qubits in Industry-Standard SOI Technology

Marc Sanquer et al., 2017

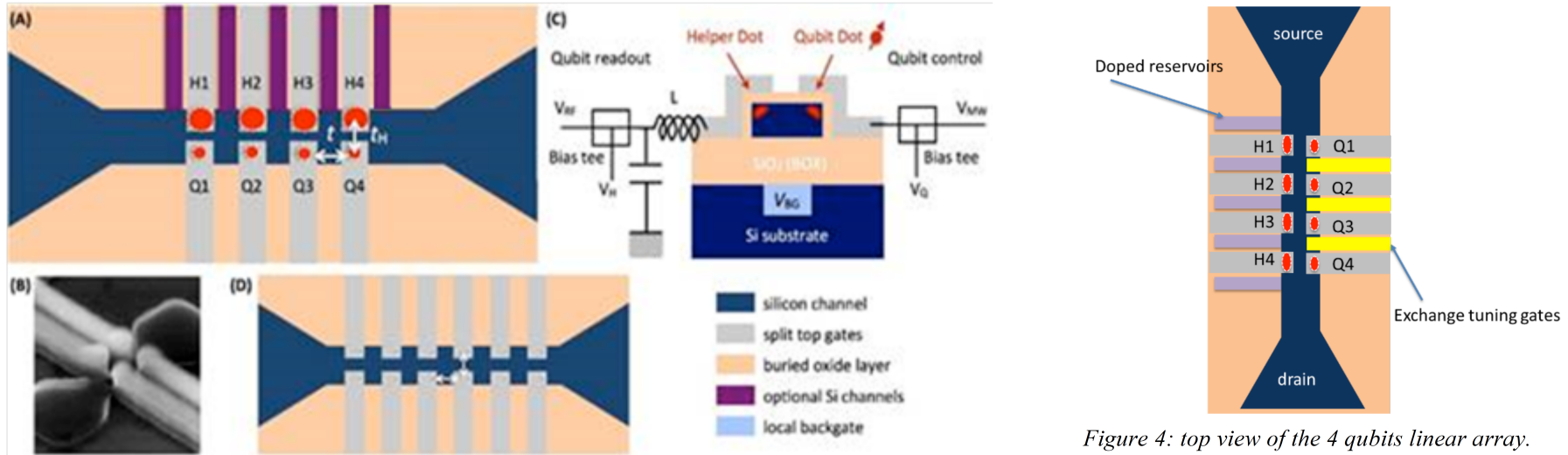


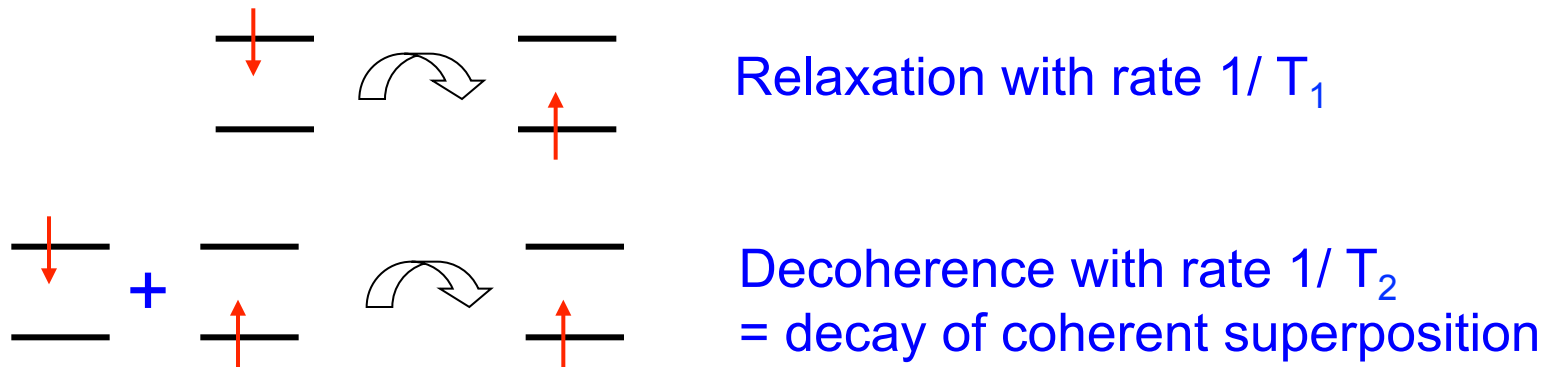
Figure 4: top view of the 4 qubits linear array.

Fig. 1. a) Schematic of the targeted 4x2 linear array of SOI quantum dots. b) SEM top view of current 2x2 split gate with gate spacing of 30 nm. c) Schematic cross-section showing the corner dots located under the slit gates. Their coupling can be tuned by using local back gate voltage ( $V_{BG}$ ). The qubit dot is operated using microwaves ( $V_{MW}$ ), whereas the helper dot is probed by rf signals ( $V_{RF}$ ) for qubit readout. d) Scalable architecture envisioned based on our approach.

# Spin decoherence in GaAs quantum dots

Two important sources of spin decay in GaAs:

- 1) Spin-orbit interaction (Dresselhaus & Rashba)  
→ interaction between spin and charge fluctuations



- 2) Hyperfine interaction between electron spin and nuclear spins, can lead to non-exponential decay

## General spin Hamiltonian:

$$H = g\mu_B \mathbf{S} \cdot \mathbf{B} + \mathbf{S} \cdot \mathbf{h}(t)$$

where  $\mathbf{h}(t)$  is a fluctuating (internal) field with  $\langle \mathbf{h}(t) \rangle = 0$

Relaxation ( $T_1$ ) and decoherence ( $T_2$ ) times in weak coupling approx.:

$$\frac{1}{T_1} = \int_{-\infty}^{\infty} dt \operatorname{Re} [\langle h_X(0)h_X(t) \rangle + \langle h_Y(0)h_Y(t) \rangle] e^{-iE_Z t/\hbar}$$

$$\frac{1}{T_2} = \frac{1}{2T_1} + \int_{-\infty}^{\infty} dt \operatorname{Re} \langle h_Z(0)h_Z(t) \rangle$$

[if  $\langle h_i(t) h_j(t') \rangle \sim \delta_{ij}$ ,  
 $i,j=(X,Y,Z)$ ]

relaxation  
contribution

<<  
'typically'

dephasing  
contribution

See e.g. Abragam

## General spin Hamiltonian:

$$H = g\mu_B \mathbf{S} \cdot \mathbf{B} + \mathbf{S} \cdot \mathbf{h}(t)$$

where  $\mathbf{h}(t)$  is a fluctuating (internal) field with  $\langle \mathbf{h}(t) \rangle = 0$

For SOI linear in momentum:

$$\mathbf{h}(t) \cdot \mathbf{B} = 0$$

(unlike spin-boson model!)



$$\frac{1}{T_2} = \frac{1}{2T_1} + \int_{-\infty}^{\infty} dt \operatorname{Re} \langle h_z(0) h_z(t) \rangle$$

relaxation  
contribution

~~<<  
‘typically’~~

dephasing  
contribution

## Spin-Orbit Interaction in GaAs Quantum Dots (2DEG):

$$H_{SO} = \alpha(p_x\sigma_y - p_y\sigma_x) \quad \leftarrow \text{Rashba SOI}$$

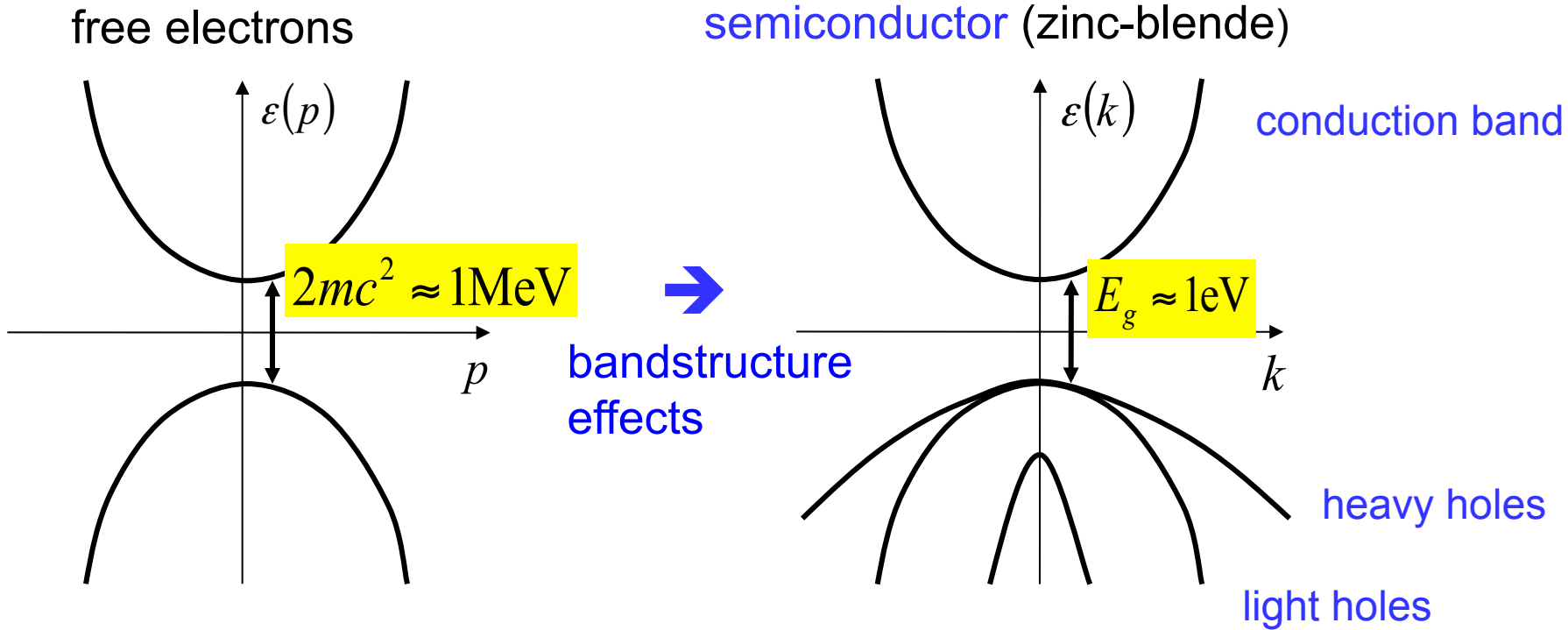
$$- \beta(p_x\sigma_x - p_y\sigma_y) \quad \leftarrow \text{Dresselhaus SOI}$$

# Basics on Spin-Orbit Interaction

Relativistic (Einstein) correction from Dirac equation:

$$H_{so} = \frac{1}{2mc^2} \vec{s} \cdot \left( \nabla V \times \frac{\vec{p}}{m} \right)$$

Thomas term ( $\rightarrow$  Rashba SOI)



# Spin-Orbit Interaction in GaAs Quantum Dots (2DEG):

$$H_{SO} = \alpha(p_x\sigma_y - p_y\sigma_x) \quad \leftarrow \text{Rashba SOI}$$

$$- \beta(p_x\sigma_x - p_y\sigma_y) \quad \leftarrow \text{Dresselhaus SOI}$$

Model Hamiltonian:

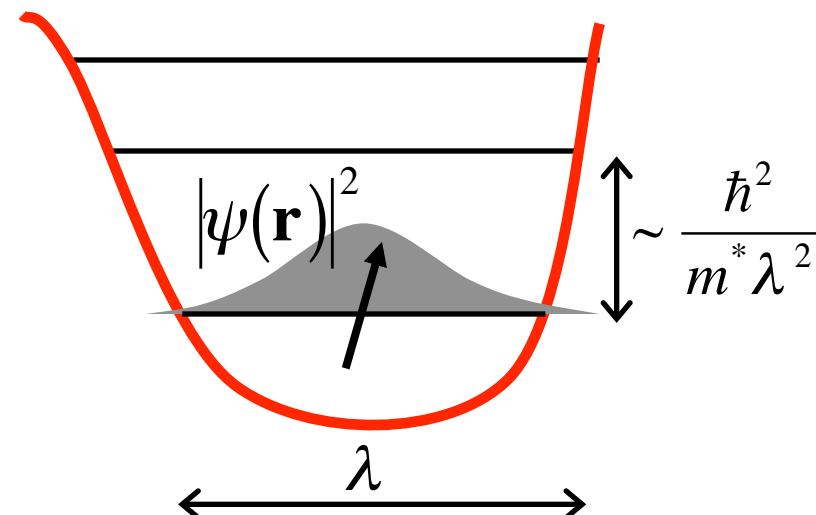
$$H = H_{dot} + H_Z + H_{SO} + U_{el-ph}(t)$$

piezoelectric & deformation  
acoustic

$$H_{dot} = \frac{p^2}{2m^*} + U(\mathbf{r}/\lambda)$$

$$H_Z = \frac{1}{2}g\mu_B \mathbf{B} \cdot \boldsymbol{\sigma}$$

$$U_{el-ph}(t) = \dots \quad \leftarrow \text{any potential fluctuation, e.g., phonons}$$



# Electron-phonon interaction (quasi-2D)

$$U_{el-ph} = \sum_{\mathbf{q},j} \frac{F(q_z) e^{i\mathbf{q}_{||}\mathbf{r}}}{\sqrt{2\rho_c \omega_{qj}/\hbar}} (e\beta_{\mathbf{q}j} - iq\Xi_{\mathbf{q}j}) (b_{-\mathbf{q}j}^+ + b_{\mathbf{q}j})$$

- piezo-electric interaction:

$$\beta_{\mathbf{q}j} = \frac{2\pi}{q^2 \kappa} \beta^{\mu\nu\varpi} q_\mu (q_\nu e_{\varpi}^{(j)}(\mathbf{q}) + q_\varpi e_\nu^{(j)}(\mathbf{q})) \quad \mathbf{q} = (\mathbf{q}_{||}, q_z)$$

- deformation potential interaction:

$$\Xi_{\mathbf{q}j} = \frac{1}{2q} \Xi^{\mu\nu} (q_\mu e_\nu^{(j)}(\mathbf{q}) + q_\nu e_\mu^{(j)}(\mathbf{q}))$$

for GaAs:  $\Xi_{\mathbf{q}j} = \Xi_0 \delta_{j,1}$  and  $\beta^{\mu\nu\varpi} = \begin{cases} h_{14}, & \mu\nu\varpi = xyz \text{ (cyclic)} \\ 0, & \text{otherwise} \end{cases}$

Quantum well form-factor  $F(q_z)$ :

$$F(q_z) = \int dz e^{iq_z z} |\psi(z)|^2$$

- parabolic quantum well:

$$\psi(z) = \pi^{-1/4} d^{-1/2} e^{-z^2/2d^2} \Rightarrow F(q_z) = e^{-q_z^2 d^2 / 4}$$

- rectangular quantum well ( $0 < z < d$ ):

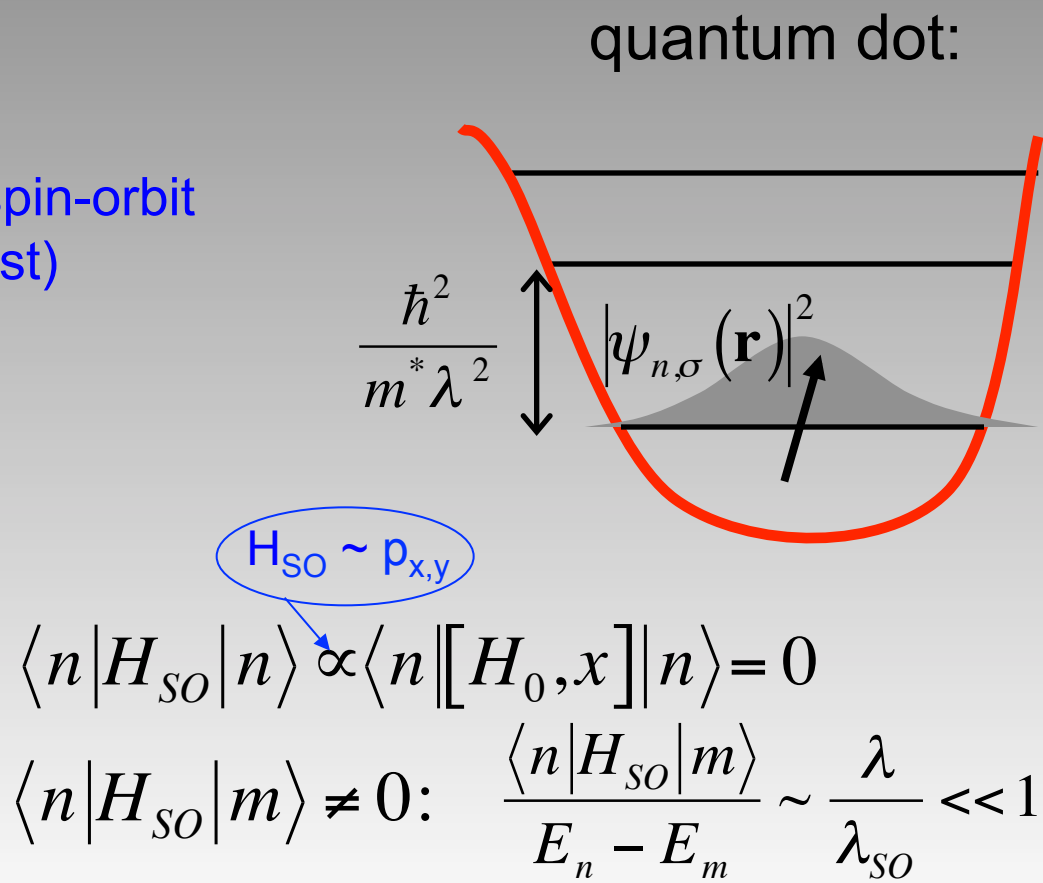
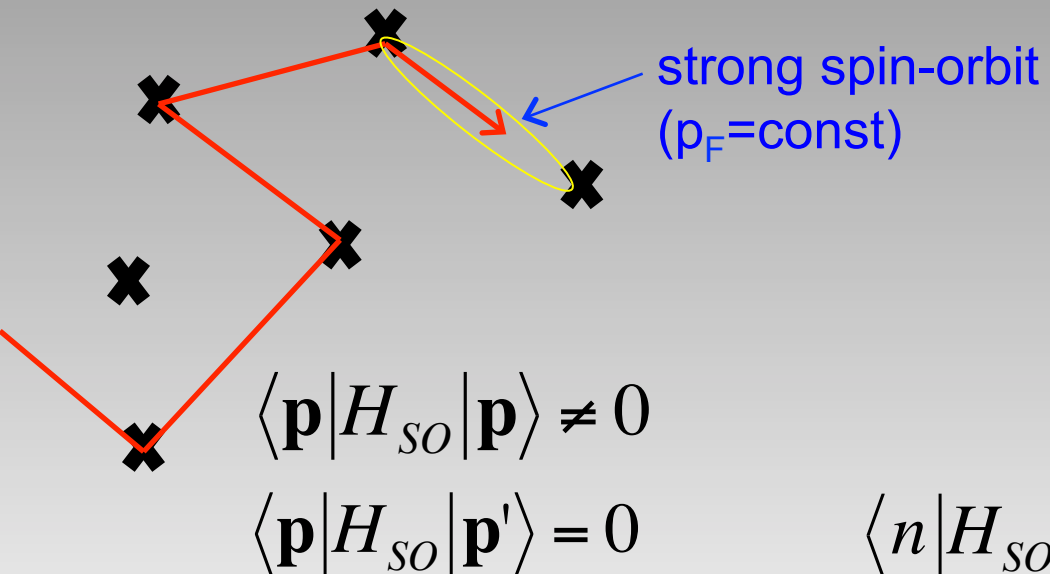
$$\psi(z) = \sqrt{\frac{2}{d}} \sin \frac{\pi z}{d} \Rightarrow F(q_z) = \frac{e^{iq_z d} - 1}{iq_z d} \frac{1}{1 - (q_z d / 2\pi)^2}$$

- triangular quantum well (Fang-Howard approx.):

$$\psi(z) = \sqrt{\frac{b^3}{2}} z e^{-zb/2}, \quad b = \left( \frac{33e^2 m^* n_0}{8\hbar^2 \epsilon \epsilon_0} \right)^{1/3}, \Rightarrow F(q_z) = \frac{1}{(1 - iq_z/b)^3}$$

## Parameter regime:

1.  $\lambda \ll \lambda_{SO}$ ,  $\lambda_{SO} = \hbar/m^*\beta$  (typically:  $\lambda \sim 100$  nm, and  $\lambda_{SO} \sim 1-10$   $\mu\text{m}$ )
2. spin-orbit interaction in quantum dot is **weak**
3.  $g\mu_B B \ll \hbar^2/m^*\lambda^2$



Parameter regime:

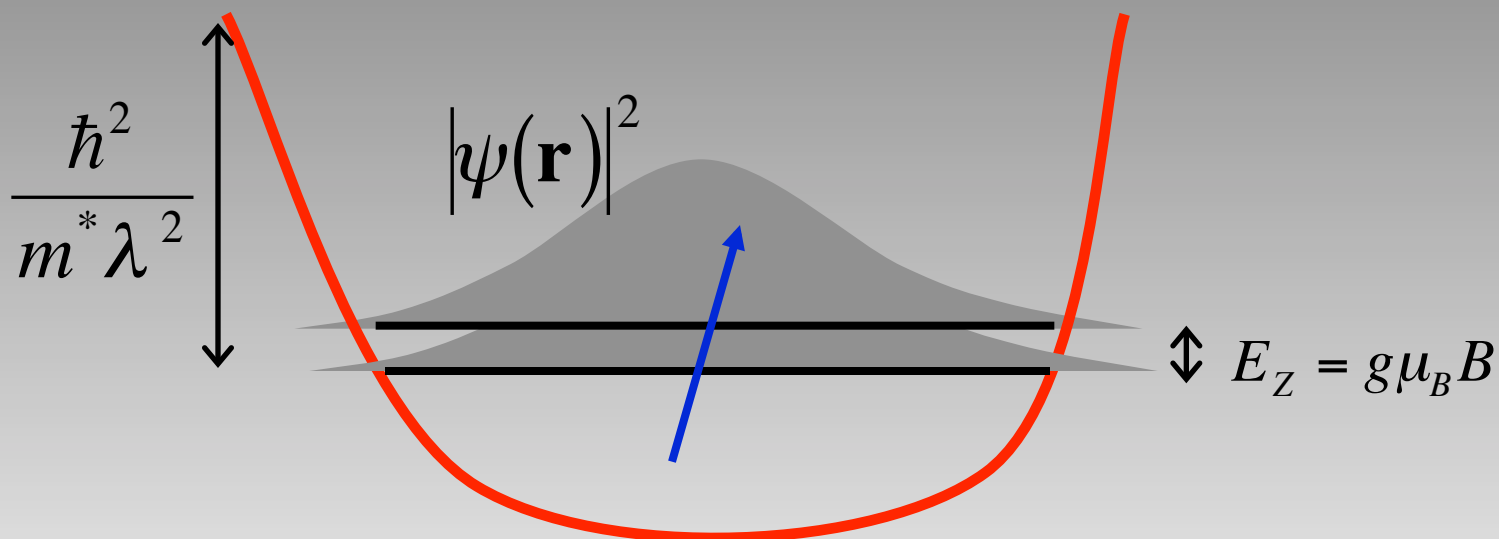
$$\lambda \ll \lambda_{SO}, \quad \lambda_{SO} = \hbar/m^* \beta$$

(typically:  $\lambda \sim 100$  nm, and  $\lambda_{SO} \sim 1-10$   $\mu\text{m}$ )

$$k_B T \ll \hbar^2/m^* \lambda^2$$

(typically:  $\hbar^2/m^* \lambda^2 \sim 1$  meV  $\approx 10$  K)

the dot stays in its orbital ground state



*Spin = Kramers doublet of ground state*

## Derivation via Schrieffer-Wolff transformation \*):

$$H = H_{dot} + H_Z + H_{SO} + U_{el-ph}(t)$$

$$\tilde{H} = e^S H e^{-S} \approx H_d + H_Z + U_{el-ph}(t) + [S, U_{el-ph}(t)]$$

unitary trafo removes  
1st order in  $H_{SO}$

with  $S$  defined by  $[H_d + H_Z, S] \equiv (\hat{L}_d + \hat{L}_Z)S = H_{SO}$

Liouville superoperators

with  $p_x = im^*[H_d, x]$ , get  $H_{SO} = i[H_d, \sigma \cdot \xi] \equiv i\hat{L}_d \sigma \cdot \xi$

thus:  $S = \frac{1}{\hat{L}_d + \hat{L}_Z} i\hat{L}_d \sigma \cdot \xi = \left( \frac{1}{\hat{L}_d} - \frac{\hat{L}_Z}{\hat{L}_d^2} + \dots \right) i\hat{L}_d \sigma \cdot \xi = S^{(0)} + S^{(1)} + \dots$

$$S^{(0)} = i\sigma \cdot \xi, \quad H_d |n\rangle = E_n |n\rangle$$

no orbital B-effect to  $O(H_{SO})$ :  $[S^{(0)}, U_{el-ph}(t)]_{nn} = [i\sigma \cdot \xi, U_{el-ph}(t)]_{nn} = 0$

\*) Bravyi, DiVincenzo, and DL, Annals of Physics 326, 2793-2826 (2011)

leading order is due to Zeeman term (no orbital):

$$S^{(1)} = -\frac{1}{\hat{L}_d} \hat{L}_z i \sigma \cdot \xi = g \mu_B \sigma \cdot \left[ \mathbf{B} \times \left( \frac{1}{\hat{L}_d} \xi \right) \right],$$

giving  $H_{\text{eff}} = \langle \psi | \tilde{H} | \psi \rangle + \text{spin-independent constant}$

$$H_{\text{eff}} = \frac{1}{2} g \mu_B (\mathbf{B} + \delta \mathbf{B}(t)) \cdot \boldsymbol{\sigma}, \quad \delta \mathbf{B}(t) = 2 \mathbf{B} \times \boldsymbol{\Omega}(t),$$

where  $\boldsymbol{\Omega}(t) = \langle \psi | [\hat{L}_d^{-1} \xi, U_{el-ph}(t)] | \psi \rangle \propto \lambda / \lambda_{SO}$ ,

$$\xi = (y'/\lambda_-, x'/\lambda_+, 0), \quad 1/\lambda_{\pm} = m^*(\beta \pm \alpha)/\hbar, \quad \begin{cases} x' = (x+y)/\sqrt{2} \\ y' = -(x-y)/\sqrt{2} \end{cases}$$

## Parameter regime:

1.  $\lambda \ll \lambda_{SO}$ ,  $\lambda_{SO} = \hbar/m^* \beta$  (typically:  $\lambda \sim 100$  nm, and  $\lambda_{SO} \sim 1-10$  μm)
2.  $k_B T \ll \hbar^2/m^* \lambda^2$  (typically:  $\hbar^2/m^* \lambda^2 \sim 1$  meV  $\approx 10$  K)
3.  $g\mu_B B \ll \hbar^2/m^* \lambda^2$

In this regime, we find effective spin Hamiltonian ( $\sim H_{SO}, U_{e-ph}$ ):

$$H_{\text{eff}} = \frac{1}{2} g\mu_B (\mathbf{B} + \delta\mathbf{B}(t)) \cdot \boldsymbol{\sigma},$$

$$\delta\mathbf{B}(t) = 2\mathbf{B} \times \boldsymbol{\Omega}(t),$$

→ no dephasing!  
i.e.  $T_2 = 2T_1$

Golovach, Khaetskii & DL, PRL 93 (2004)

where  $\boldsymbol{\Omega}(t) = \langle \psi | [\hat{L}_d^{-1} \xi, U_{el-ph}(t)] | \psi \rangle$ ,

$$\xi = (y'/\lambda_-, x'/\lambda_+, 0),$$

$$1/\lambda_{\pm} = m^*(\beta \pm \alpha)/\hbar,$$

$$\begin{cases} x' = (x+y)/\sqrt{2} \\ y' = -(x-y)/\sqrt{2} \end{cases}$$

## Bloch Equations (Born approx. in $\delta B$ ):

$$\langle \dot{\mathbf{S}} \rangle = g\mu_B \mathbf{B} \times \langle \mathbf{S} \rangle - \Gamma \langle \mathbf{S} \rangle + \mathbf{Y}$$

(spin: Kramers doublet)

$\tau_c = \lambda / s = 100 \text{ ps} \ll T_{1,2}$   
 & super-Ohmic spectrum }  $\rightarrow$  Born-Markov approx. ok

Decay tensor:

$$\Gamma_{ij} \propto J_{ij}(w) = \frac{g^2 \mu_B^2}{2\hbar^2} \int_0^\infty \langle \delta B_i(0) \delta B_j(t) \rangle e^{-iwt} dt$$

spectral function

decay:  $\Gamma = \Gamma^r + \Gamma^d$ ,

relaxation:  $\Gamma_{ij}^r = \delta_{ij} (\delta_{pq} - l_p l_q) J_{pq}^+(\omega) - (\delta_{ip} - l_i l_p) J_{pj}^+(\omega) - \delta_{ij} \epsilon_{kpq} l_k I_{pq}^-(\omega) + \epsilon_{ipq} l_p I_{qj}^-(\omega)$ ,

dephasing:  $\Gamma_{ij}^d = \delta_{ij} l_p l_q J_{pq}^+(0) - l_i l_p J_{pj}^+(0) \rightarrow 0$

$$J_{ij}^\pm(w) = \operatorname{Re} [J_{ij}(w) \pm J_{ij}(-w)], \quad I_{ij}^\pm(w) = \operatorname{Im} [J_{ij}(w) \pm J_{ij}(-w)]$$

## Relaxation rate:

$$\frac{1}{T_1} \propto \text{Re } J_{XX}(z) = \frac{\omega^2 z^3 (2n_z + 1)}{(2\Lambda_+ m^* \omega_0^2)^2} \sum_j \frac{\hbar}{\pi \rho_c s_j^5} \int_0^{\pi/2} d\theta \sin^3 \theta$$

**Bose function**

$$x e^{-(z\lambda \sin \theta)^2 / 2s_j^2} \left| F\left(\frac{|z|}{s_j} \cos \theta\right) \right|^2 \left( e^2 \overline{\beta_{j\theta}^2} + \frac{z^2}{s_j^2} \overline{\Xi_j^2} \right) \propto \lambda^2 / \lambda_{SO}^2$$

↑                      ↑                      ↑

**quantum well**      **piezo**      **deformation**

$$z \rightarrow \omega = g\mu_B B$$

Golovach, Khaetskii, Loss, PRL 93 (2004)

$$\frac{2}{\Lambda_\pm^2} = \frac{1 - l_{x'}^2}{\lambda_-^2} + \frac{1 - l_{y'}^2}{\lambda_+^2} \pm \sqrt{\left( \frac{1 - l_{x'}^2}{\lambda_-^2} + \frac{1 - l_{y'}^2}{\lambda_+^2} \right)^2 - \frac{4l_z^2}{\lambda_+^2 \lambda_-^2}}$$

**effective SO length**

# Relaxation rate:

Bose function      super-Ohmic:  $\sim z^3$

$$\frac{1}{T_1} \propto \operatorname{Re} J_{XX}(z) = \frac{\omega^2 z^3 (2n_z + 1)}{(2\Lambda_+ m^* \omega_0^2)^2} \sum_j \frac{\hbar}{\pi \rho_c s_j^5} \int_0^{\pi/2} d\theta \sin^3 \theta$$

$$x e^{-(z\lambda \sin \theta)^2 / 2s_j^2} \left| F\left(\frac{|z|}{s_j} \cos \theta\right) \right|^2 \left( e^2 \overline{\beta_{j\theta}^2} + \frac{z^2}{s_j^2} \overline{\Xi_j^2} \right) \propto \lambda^2 / \lambda_{SO}^2$$

$z \rightarrow \omega = g\mu_B B$       quantum well      piezo      deformation

$s_1 \approx 4.7 \times 10^3 \text{ m/s}$ ,  $s_2 = s_3 \approx 3.37 \times 10^3 \text{ m/s}$       speed of sound

$$\sqrt{\Xi_j^2} = \delta_{j,1} \Xi_0, \quad \Xi_0 \approx 7 \text{ eV}, \quad \sqrt{\beta_{1,\vartheta}^2} = 3\sqrt{2}\pi h_{14} \kappa^{-1} \sin^2 \vartheta \cos \vartheta, \quad \sqrt{\beta_{2,\vartheta}^2} = \sqrt{2}\pi h_{14} \kappa^{-1} \sin 2\vartheta,$$

$$\sqrt{\beta_{3,\vartheta}^2} = 3\sqrt{2}\pi h_{14} \kappa^{-1} (3\cos^2 \vartheta - 1) \sin \vartheta, \quad h_{14} \approx 0.16 \text{ C/m}^2, \quad \kappa \approx 13$$

$$\frac{2}{\Lambda_\pm^2} = \frac{1-l_{x'}^2}{\lambda_-^2} + \frac{1-l_{y'}^2}{\lambda_+^2} \pm \sqrt{\left( \frac{1-l_{x'}^2}{\lambda_-^2} + \frac{1-l_{y'}^2}{\lambda_+^2} \right)^2 - \frac{4l_z^2}{\lambda_+^2 \lambda_-^2}}$$

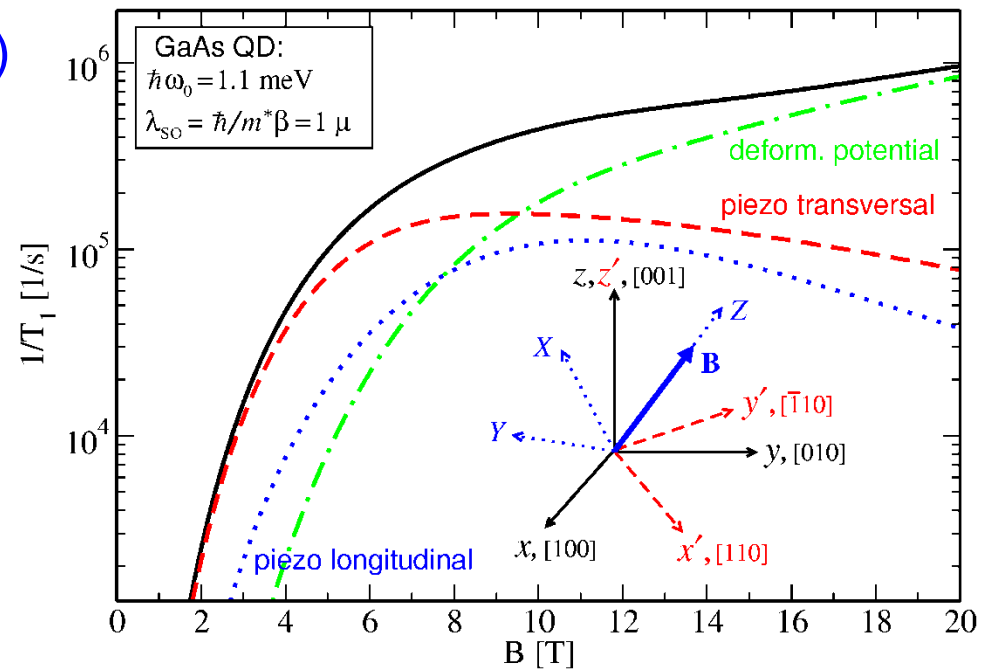
effective SO length

# Spin relaxation rate $1/T_1$ for GaAs quantum dot

$$\frac{1}{T_1} \propto (g\mu_B B)^2 + \nu_{ph}(\omega) \propto \omega^2 + H_{SO} \propto p_\alpha \times \int_0^{\pi/2} d\theta \sin^k \theta e^{-(g\mu_B B \lambda \sin \theta)^2 / 2s_j^2}$$

$\delta B^2 \propto B^2$

power-5 law for  $B < 3T$  (GaAs)



## Numerical value of $T_1$ for GaAs parameters (13!):

$$\left( \hbar\omega_0, \lambda, d, \lambda_{SO} = \hbar/m^* \beta, \alpha, \kappa, \Xi_0, h_{14}, s_1, s_2 = s_3, \rho_c, m^* \right) = \\ \left( 1.1 \text{meV}, 32 \text{nm}, 5 \text{nm}, 9 \mu\text{m}, 0, 13.1, 6.7 \text{eV}, 0.16 \text{C/m}^2, \right. \\ \left. 4.73 \times 10^5 \text{cm/s}, 3.35 \times 10^5 \text{cm/s}, 5.3 \times 10^3 \text{kg/m}^3, 0.067 m_e \right)$$

Zumbuhl ea PRL 89 (276803) 2003

$$|g| = 0.43 \pm 0.04 - (0.0077 \pm 0.0020)B(T)$$

or with linear fit:  $|g| = 0.29$  Hanson ea PRL 91 (196802) 2003

Theory:

$$T_1 \approx 750 \text{ }\mu\text{s}, \text{ for } B = 8\text{T}$$

$$\propto \lambda_{SO}^{-2} / \lambda^2$$

$T_1 = 550 - 1100 \text{ }\mu\text{s}$  due to uncertainties in  $g$  factor

$T_1 = 2.7 \text{ ms}$  for  $\lambda_{SO} = 17 \mu\text{m}$  [Huibers ea PRL 83, 5090 (1999)]

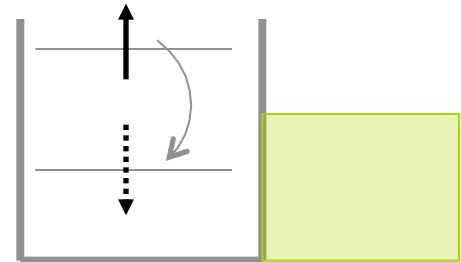
Experiment:

$$T_1^{\text{exp.}} = 800 \text{ }\mu\text{s} @ 8T$$

Elzerman *et al.*,  
Nature 430, 431 (2004)

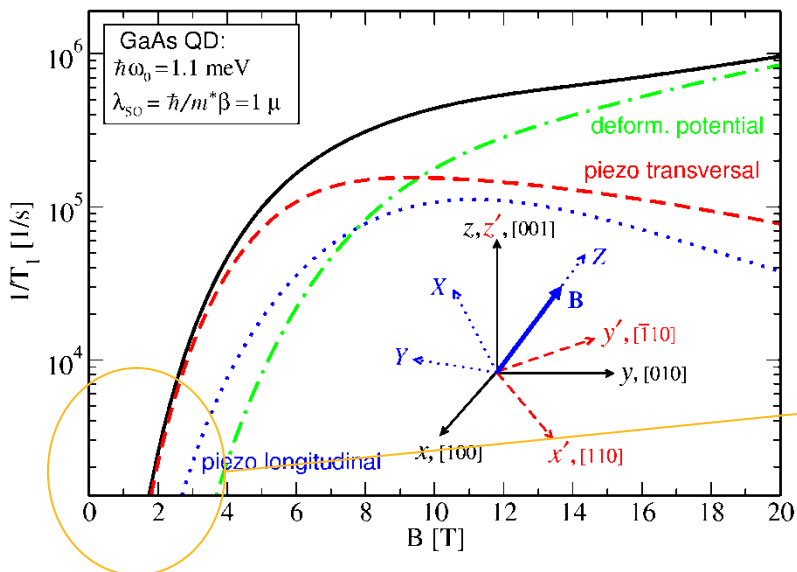
# Read-out via spin-charge conversion:

DL&DiVincenzo 1998



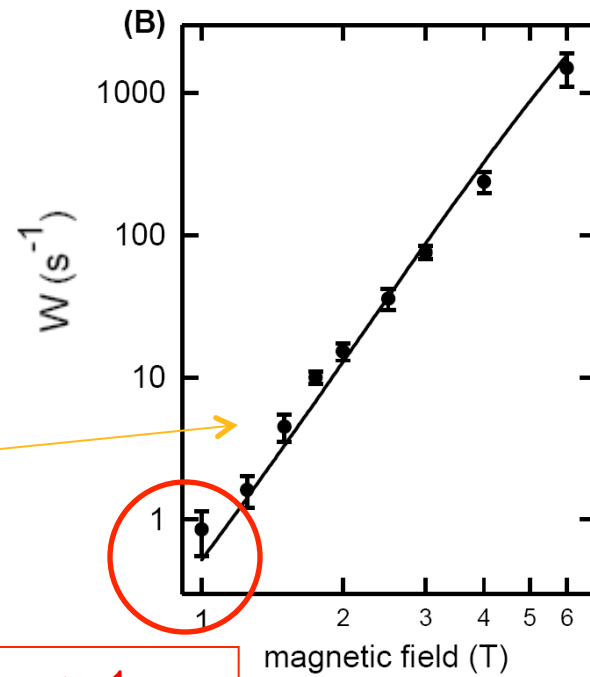
## spin relaxation rates $1/T_1$ :

Theory: Basel, 2004



→ prediction confirmed

Experiment: MIT 2008



Golovach, Khaetskii, DL, PRL '04

Amasha, Zumbuhl, et al., PRL '08

$1/T_{1,2}$  depends strongly on B-field direction (“magic angles”):

$$\frac{1}{T_1} = \frac{f(\varphi, \theta, \alpha)}{T_1(\theta = \pi/2, \alpha = 0)}$$

Golovach, Khaetskii, Loss  
PRL 93, 016601 (2004);  
PRB 77, 045328 (2008)

$$f(\varphi, \theta, \alpha) = \frac{1}{\beta^2} \left[ (\alpha^2 + \beta^2) (1 + \cos^2 \theta) + 2\alpha\beta \sin^2 \theta \sin 2\varphi \right]$$

“ellipsoid”

Rashba and Dresselhaus interfere! \*)

Special case:

$$\alpha = \beta, \quad \theta = \pi/2, \quad \varphi = 3\pi/4 \quad \rightarrow \quad T_1 \rightarrow \infty$$

exact!

\*) Schliemann, Egues, and DL, PRL `03

$1/T_{1,2}$  depends strongly on B-field direction (“magic angles”):

$$\frac{T}{T_1} = \frac{f(\varphi, \theta, \alpha)}{T_1(\theta = \pi/2, \alpha = 0)}$$

Golovach, Khaetskii, Loss  
PRL 93, 016601 (2004)

*Experiment ?!*

$f(\varphi, \theta, \alpha) = \frac{1}{\beta^2} [(\alpha^2 + \beta^2)(1 + \cos^2 \theta) + 2\alpha\beta \sin^2 \theta \sin 2\varphi]$

Rambo and Dresselhaus interfere! \*)

“ellipsoid”

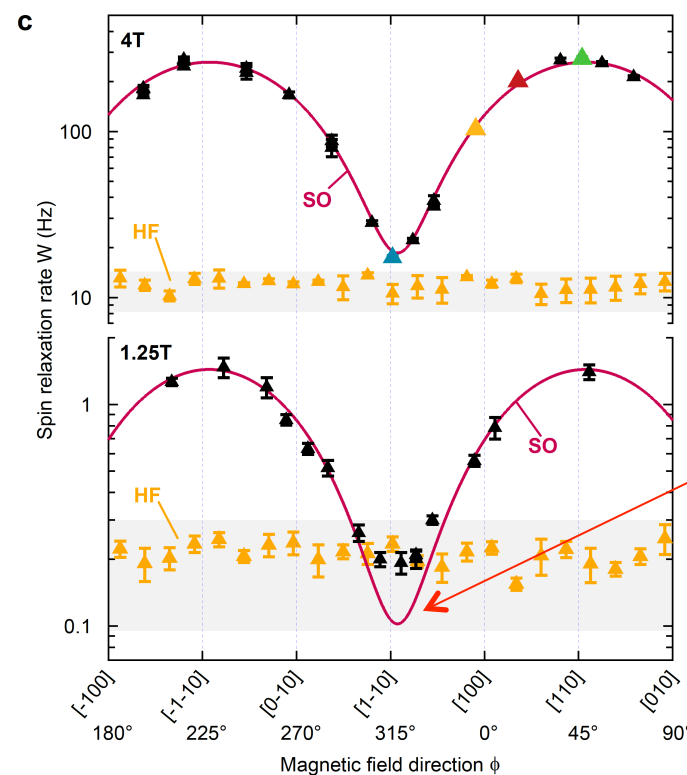
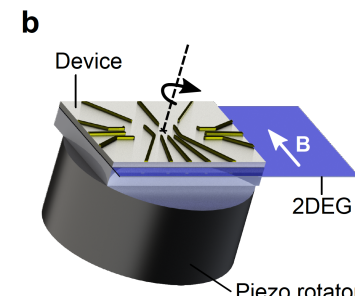
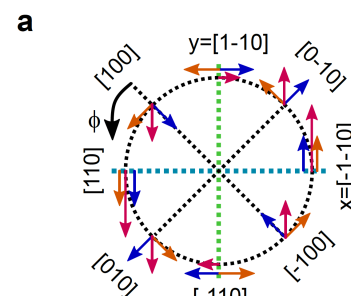
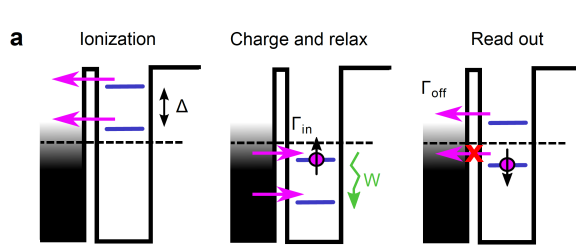
Special case:  
 $\alpha = \beta, \theta = \pi/2, \varphi = 3\pi/4$

$T_1 \rightarrow \alpha$   
exact!

\*) Schliemann, Egues, DL, PRL '03

# Ultra-long spin relaxation in a single electron GaAs quantum dot

Camenzind, Yu, Stano, Zimmerman, Gossard, Loss, and Zumbühl, preprint 2017



dominant source:  
hyperfine interaction  
with nuclear spins

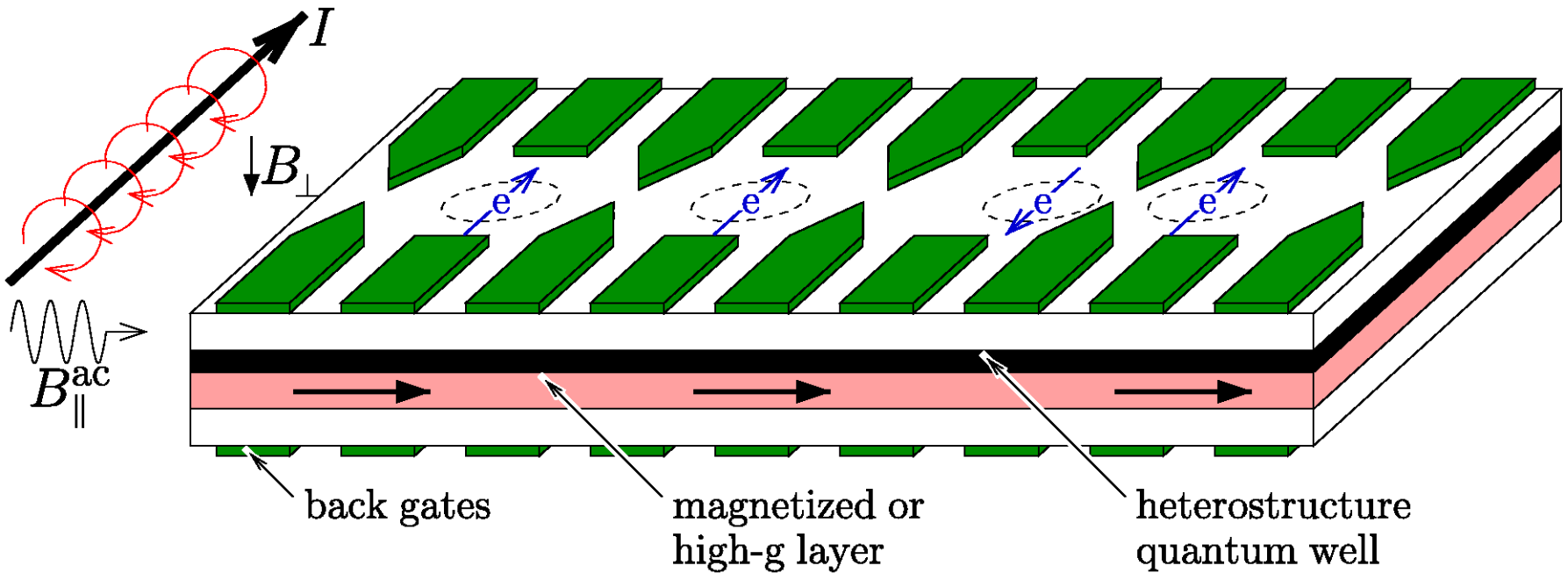
$T=60 \text{ mK}$

$T_1 \sim 1 \text{ min}$

→ current world record  
even longer than in Si:  $T_1^{\text{Si}} \sim 30 \text{ s}$ ,  
M. Simmons et al., 2017

# Scaling-up of spin qubits $\rightarrow$ quantum dot array

DL & DiVincenzo, PRA 57 (1998) 120

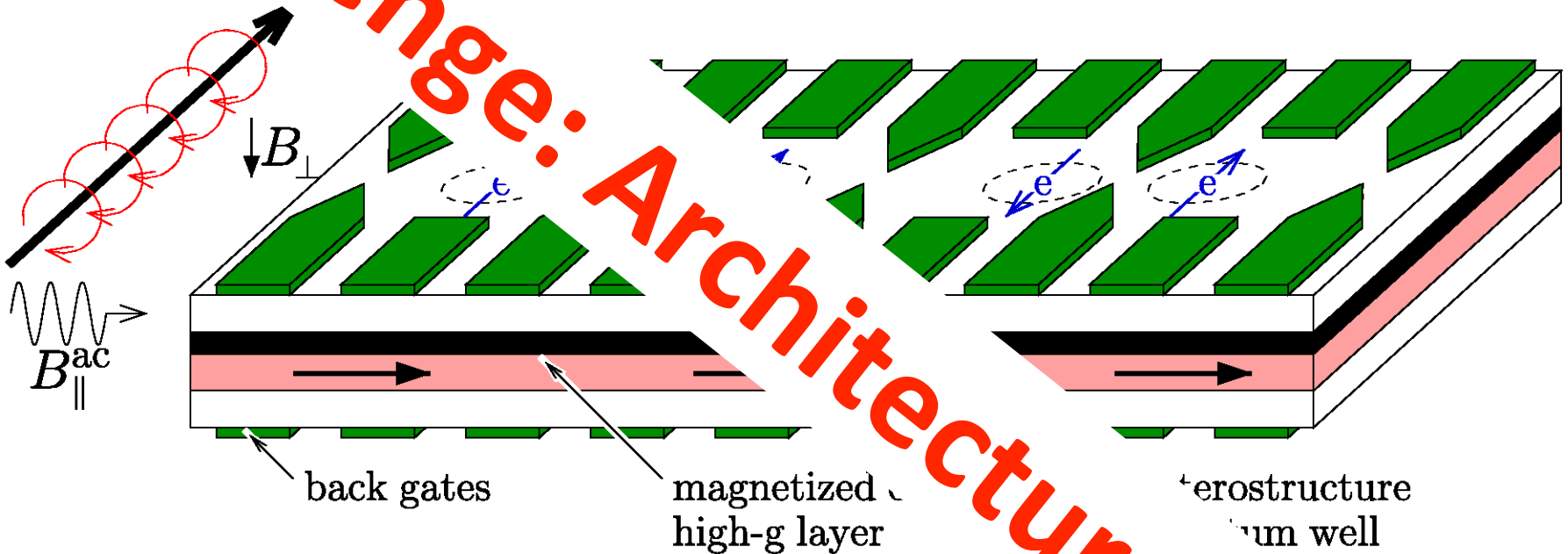


$$H = \sum_{\langle ij \rangle} J_{ij}(t) \mathbf{S}_i \cdot \mathbf{S}_j + \sum_i (g_i \mu_B \mathbf{B}_i)(t) \cdot \mathbf{S}_i$$

n.n. exchange      local Zeeman

Stringing-up of spin qubits  $\rightarrow$  quantum dot array

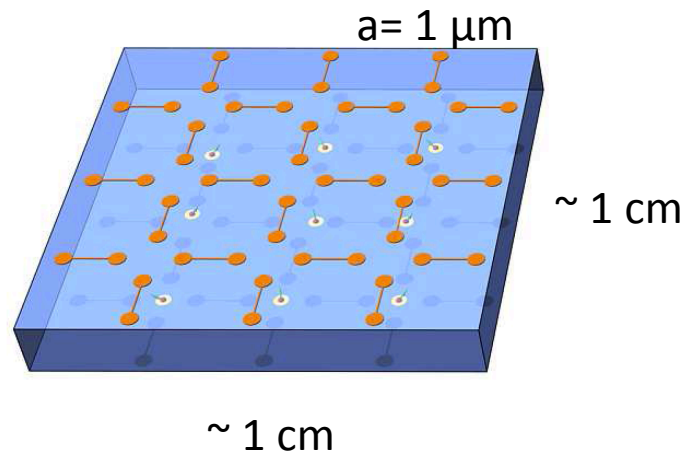
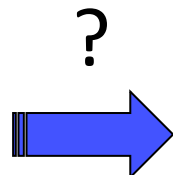
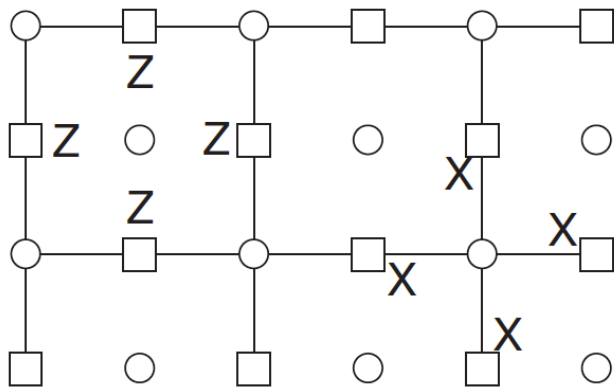
Yao & DiVincenzo, PRA 57 (1998) 120



$$H = \sum_{\langle ij \rangle} J_{ij}(t) \mathbf{S}_i \cdot \mathbf{S}_j + \sum_i (g_i \mu_B) \mathbf{B} \cdot \mathbf{S}_i$$

n.n. exchange      local Zeem.

# Quantum Chip Size in Surface Code Architecture



Bravyi and Kitaev, arXiv:quant-ph/9811052  
Raussendorf and Harrington, PRL 98,190504 (2007)

→ powerful quantum computer of size  $1 \text{ cm}^2$  with  $10^8$  spin qubits  
GHz clock-speed → can factor a 2000-bit number (RSA key) in 26h

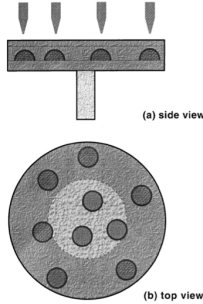
error threshold of ca. 1 % – 18 % (perfect measurement)\*

Wang, Fowler, and Hollenberg, PRA 83, 020302 (2011)

\*Error correction: Wootton and DL, PRL 109, 160503 (2012)

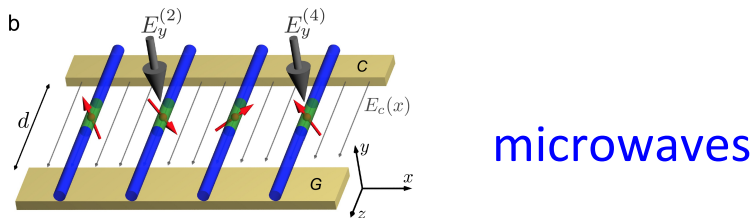
# Long-distance coupling of spin qubits

## Electromagnetic cavity & waves



Imamoglu et al.,  
PRL 83, 4204 (1999)

optical



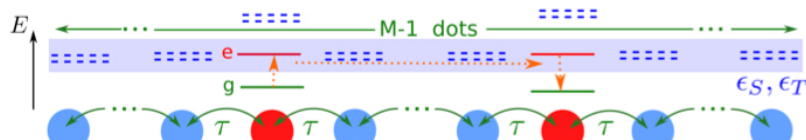
microwaves

Trif, Golovach & DL, PRB 77, 045434 (2008)

Kloeffel et al., PRB 88, 241405 (2013)

Nigg, Fuhrer, and DL, PRL 2017

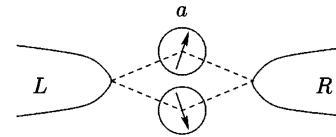
PACT



Stano et al., PRB 92, 075302 (2015)

44

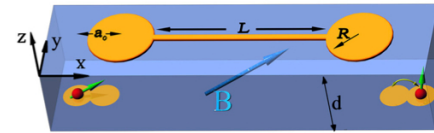
## superconductor (CAR)



$$J(r) = J_0 e^{-2r/\xi} \sin^2(k_F r)/(k_F r)^2$$

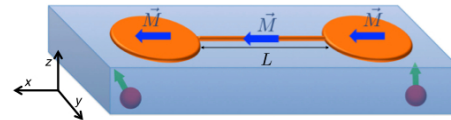
Choi, Bruder & DL, PRB 62, 13569 (2000)

## Floating metallic gate



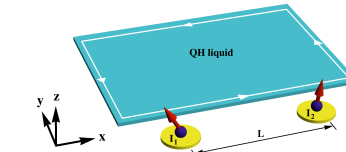
Trifunovic et al., PRX 2, 011006 (2012)

## Dipolar ferromagnet



Trifunovic et al., PRX 3, 041023 (2013)

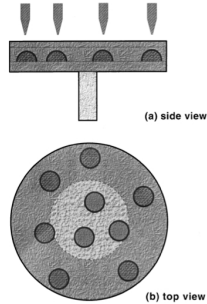
## QHE edge states



Yang et al., PRB 93, 075301 (2016)

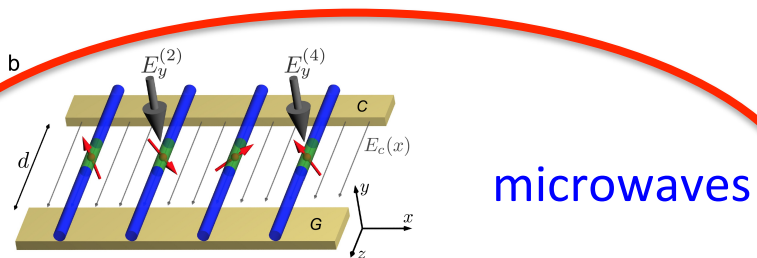
# Long-distance coupling of spin qubits

## Electromagnetic cavity & waves



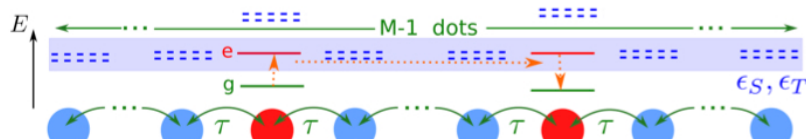
Imamoglu et al.,  
PRL 83, 4204 (1999)

optical



Trif, Golovach & DL, PRB 77, 045434 (2008)  
Kioeffel et al., PRB 88, 241405 (2013)  
Nigg, Funner, and DL, PRL 2017

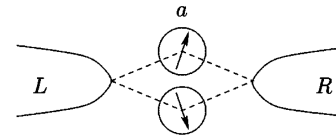
PACT



Stano et al., PRB 92, 075302 (2015)

45

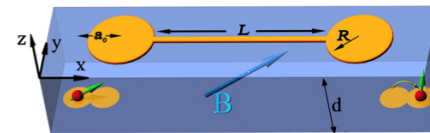
## superconductor (CAR)



$$J(r) = J_0 e^{-2r/\xi} \sin^2(k_F r)/(k_F r)^2$$

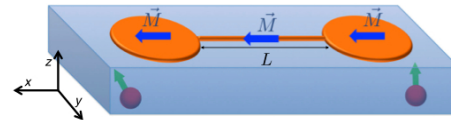
Choi, Bruder & DL, PRB 62, 13569 (2000)

Floating metallic gate



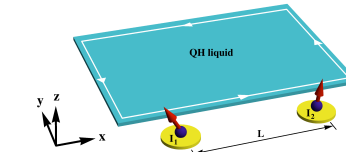
Trifunovic et al., PRX 2, 011006 (2012)

Dipolar ferromagnet



Trifunovic et al., PRX 3, 041023 (2013)

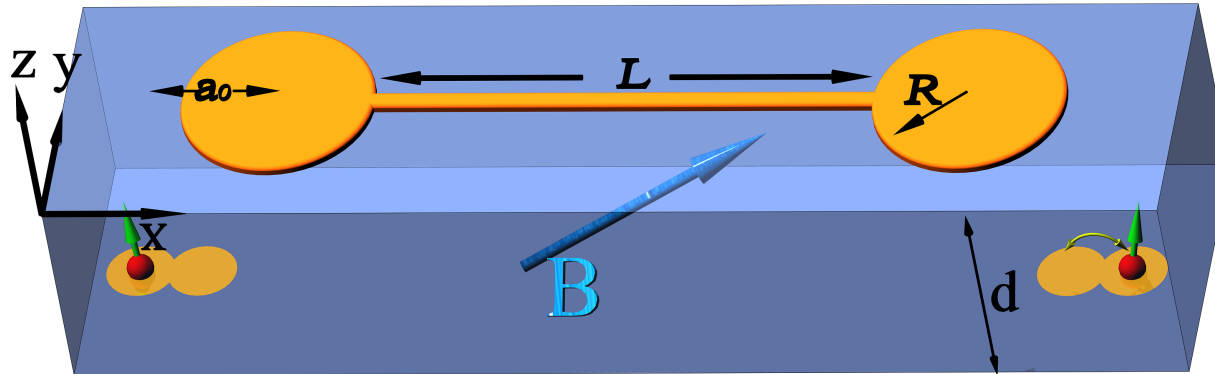
QHE edge states



Yang et al., PRB 93, 075301 (2016)

# Long-distance entanglement via floating gates

Trifunovic, Dial, Trif, Wootton, Abebe, Yacoby, DL, Phys. Rev. X 2, 011006 (2012)

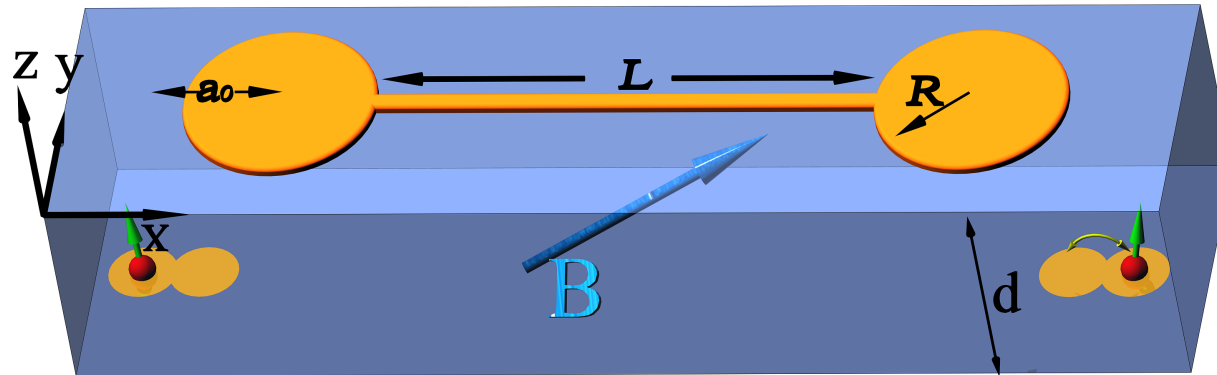


Electrostatics + spin orbit interaction → effective exchange:

$$H_{s-s} = J_x \sigma_1^x \sigma_2^x + J_y \sigma_1^y \sigma_2^y$$

# Long-distance entanglement via floating gates

Trifunovic, Dial, Trif, Wootton, Abebe, Yacoby, DL, Phys. Rev. X 2, 011006 (2012)

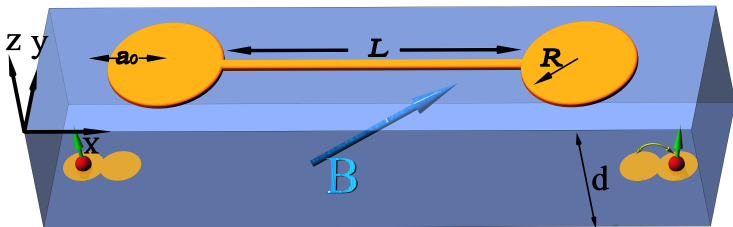


Electrostatics + spin orbit interaction → effective exchange:

$$J \simeq \frac{\pi \alpha_q \alpha_C}{4} \left( \frac{\partial q_{ind}}{\partial \tilde{x}} \right)_{r=0}^2 \left( \frac{E_Z}{\omega_x} \right)^2 \left( \frac{\lambda}{\lambda_{SO}} \right)^2 \hbar \omega_x \sim 1-100 \text{ } \mu\text{eV}$$

$$\tau_{\text{switching}} = \hbar/J \approx 1\text{ns} - 10\text{ps}$$

# Electrostatics



induced charge on gate (flat disc):

$$q_{\text{ind}}(\mathbf{r}) = \frac{2}{\pi} \arcsin(R/\xi_r),$$

$$2\xi_r^2 = R^2 + d^2 + |\mathbf{a}_0 + \mathbf{r}|^2 \\ + \sqrt{(R^2 + d^2 + |\mathbf{a}_0 + \mathbf{r}|^2)^2 - 4R^2|\mathbf{a}_0 + \mathbf{r}|^2},$$

Sten, J. Electrost. 64, 647 (2006)

Electrostatic coupling:

$$V(\mathbf{r}_1, \mathbf{r}_2) = \frac{\pi \alpha_q}{\kappa} \frac{e^2 q_{\text{ind}}(\mathbf{r}_1) q_{\text{ind}}(\mathbf{r}_2)}{R}$$

$\sim \ln(L/R_w)/L$ , for  $L \gg R$

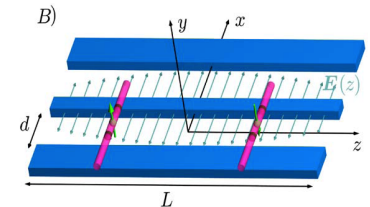
where  $\alpha_q = \frac{C_d}{C_w + 2C_d}$

$C_d = 2R/\pi,$	<b>capacitance of disc</b>
$C_w = \frac{L}{2 \ln(L/R_w)},$	<b>capacitance of wire</b>

# Long-distance Spin-Spin Coupling via Photons

Spin1-photon + Spin2-photon  $\rightarrow$  Spin1-Spin2

$$H_{s-s} = \sum_{i=1,2} \tilde{E}_{iZ}^i \sigma_z^i + J(\sigma_+^1 \sigma_-^2 + \sigma_+^2 \sigma_-^1)$$



**XY Spin-Spin Interaction – universal for quantum computing!**

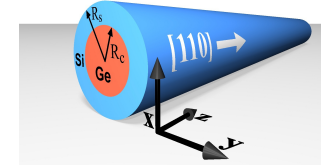
$J = \frac{\nu_{E,1}\nu_{E,2}}{2} \left( \frac{1}{\Delta_1} + \frac{1}{\Delta_2} \right)$  : effective exchange coupling – **long-range (millimeters!)**

effective Zeeman + Stark shift + Lamb shift:  $\tilde{E}_{iZ}^{eff} = E_{iZ}^{eff} + \frac{\nu_{E,i}^2}{\Delta_i} \left( n + \frac{1}{2} \right)$

detuning of the spin from the cavity mode:  $\Delta_i = E_Z^{eff} - \hbar\omega$

# Setup with Ge/Si nanowire QDs

Kloeffel, Stano, Trif, & DL, PRB 88, 241405 (2013)

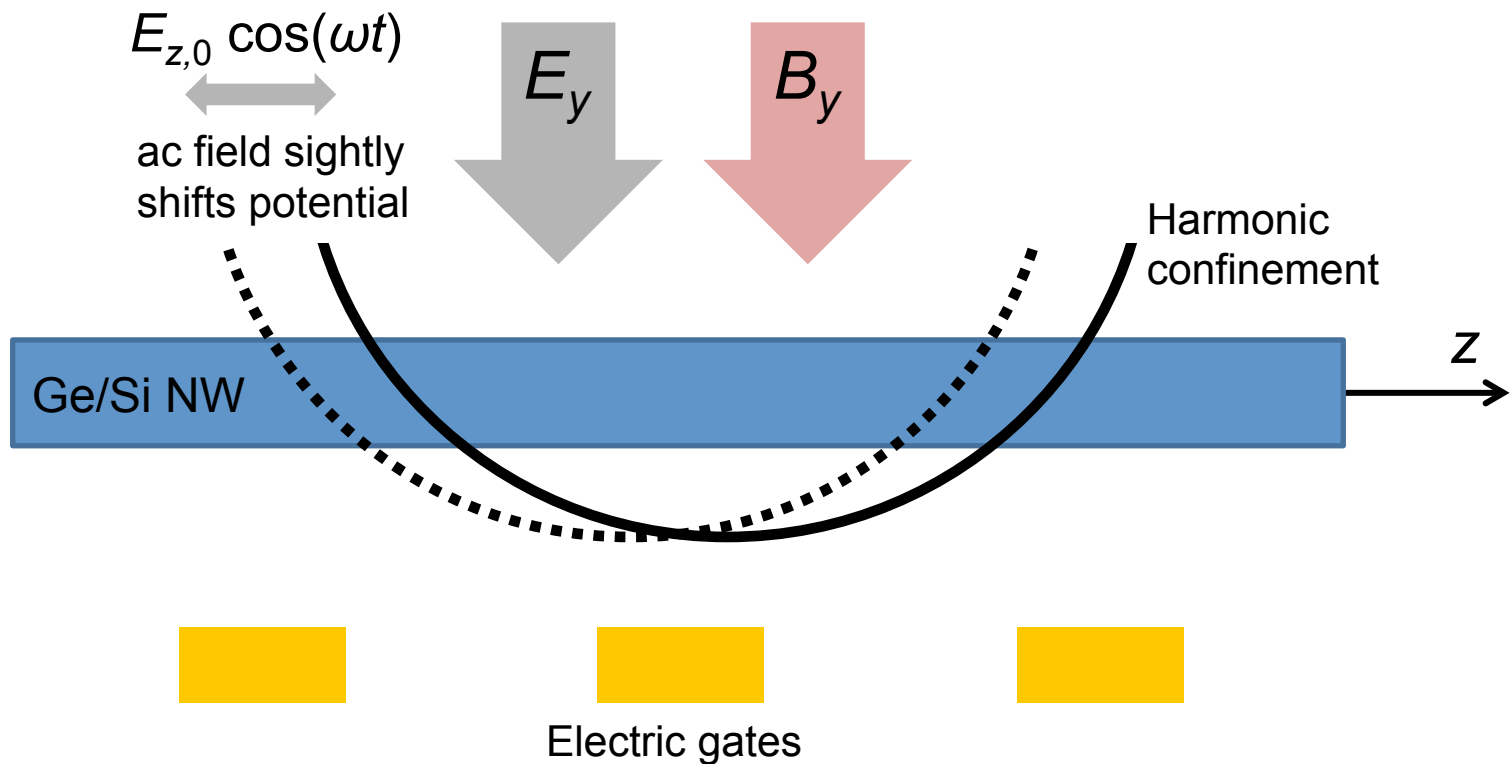


Ge/Si NWs typically have small core diameters  $\sim 10\text{--}20\text{ nm}$

→ Elongated QDs

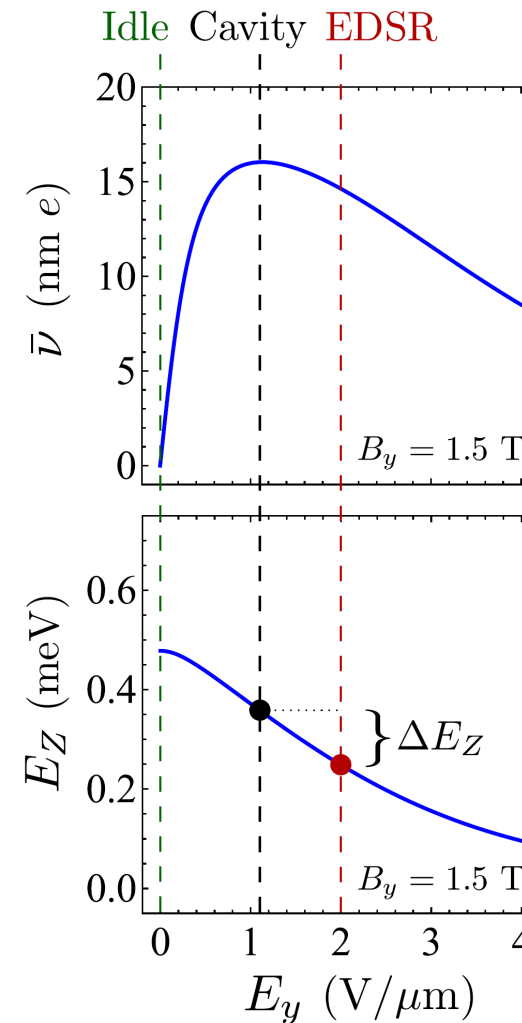
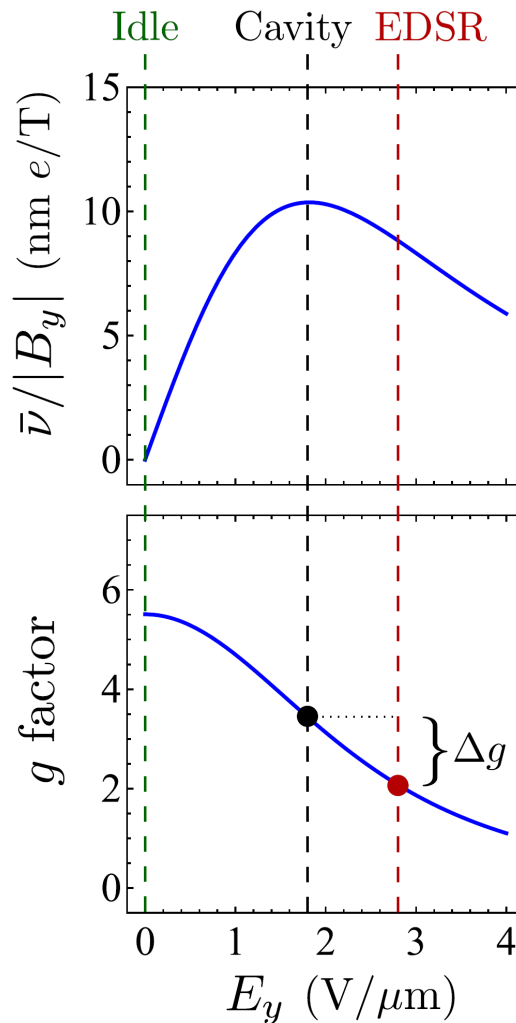
$E_y$  controls SOI  
and  $g$  factor

$B_y$  induces  
Zeeman splitting



# Single- and Two-Qubit Gates

Choosing different  $E_y$  for EDSR and cavity-mediated coupling allows independent control of single- and two-qubit operations

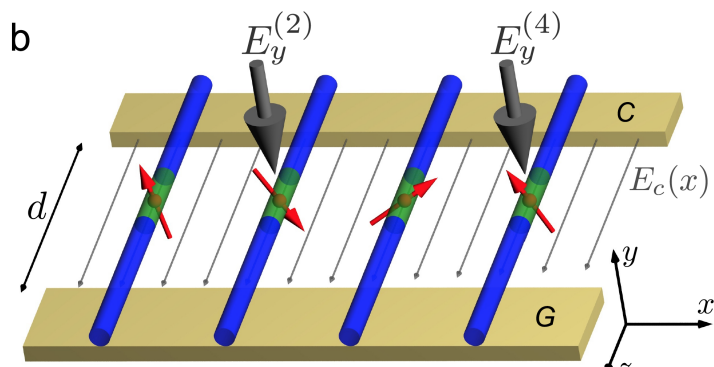


$$\begin{aligned} R &= 7.5 \text{ nm} \\ R_s &= 10 \text{ nm} \\ I_g &= 50 \text{ nm} \end{aligned}$$

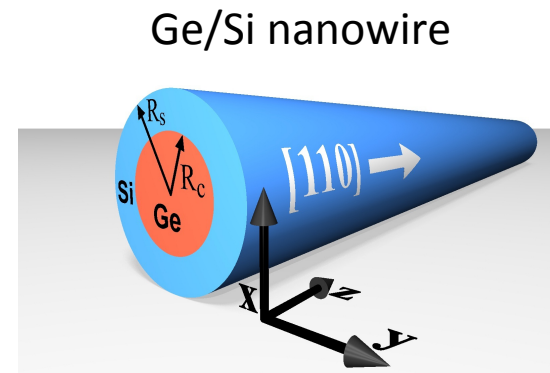
# Hole-Spin Coupling via Photons

Kloeffel, Trif, Stano, and DL, PRB 88, 241405 (2013)

hole spin  
qubits  
coupled via  
cavity mode



Wallraff *et al.*, Nature (2004)

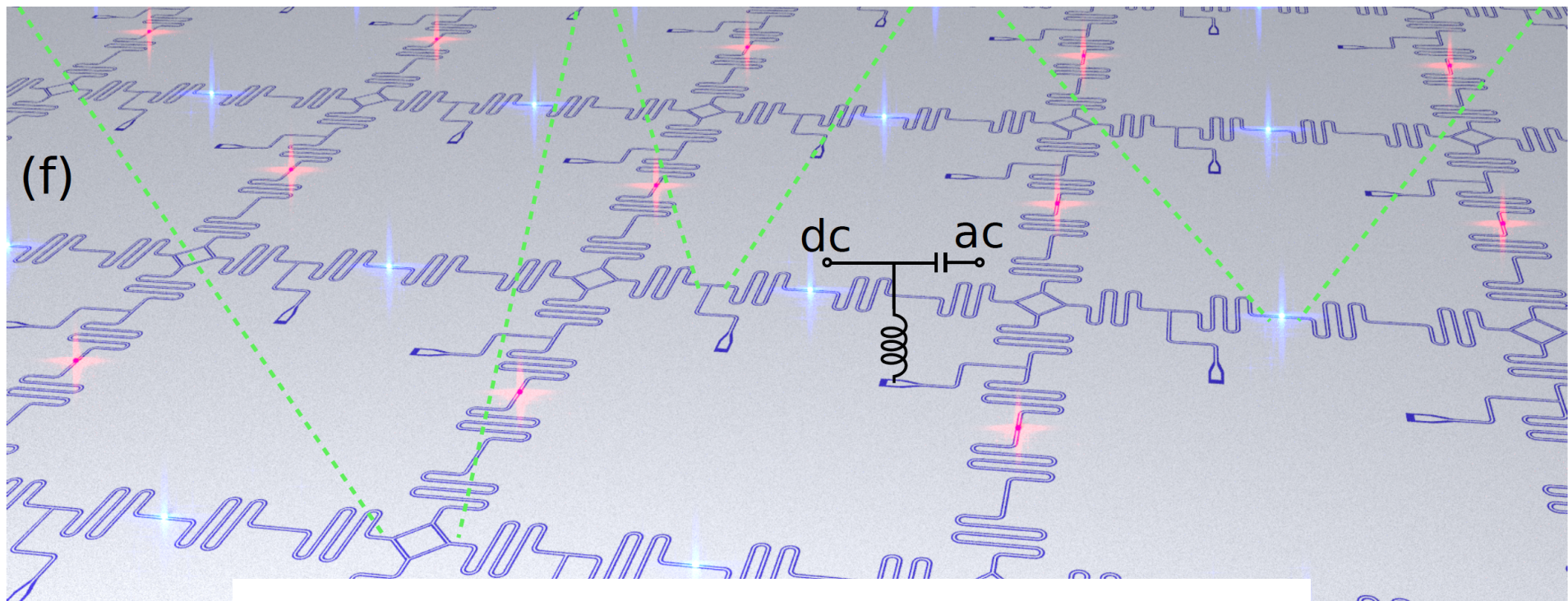


## Ultra-fast gate operation times:

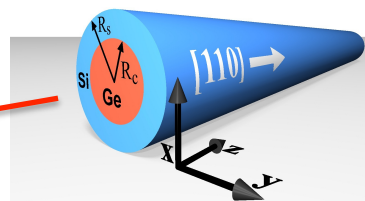
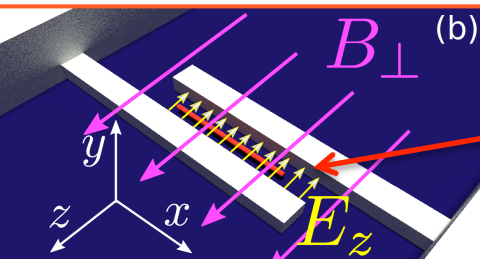
- single qubit : 40 - 100 ps
- two-qubit: 20 - 100 ns [ limited by cavity field  $E_z \sim 3V/m$  ]
- at reduced noise and large on/off ratio

# Grid-bus Surface Code with Hole Spin Qubits

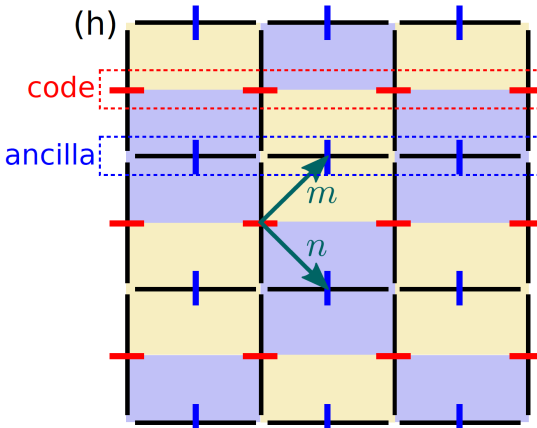
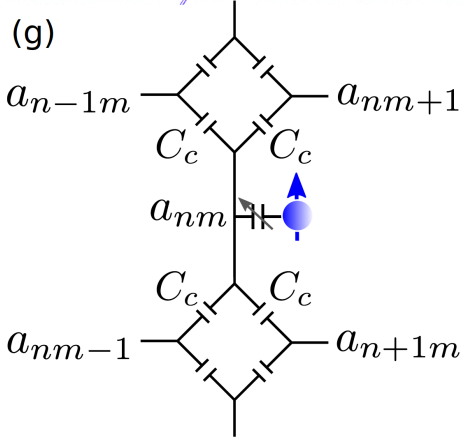
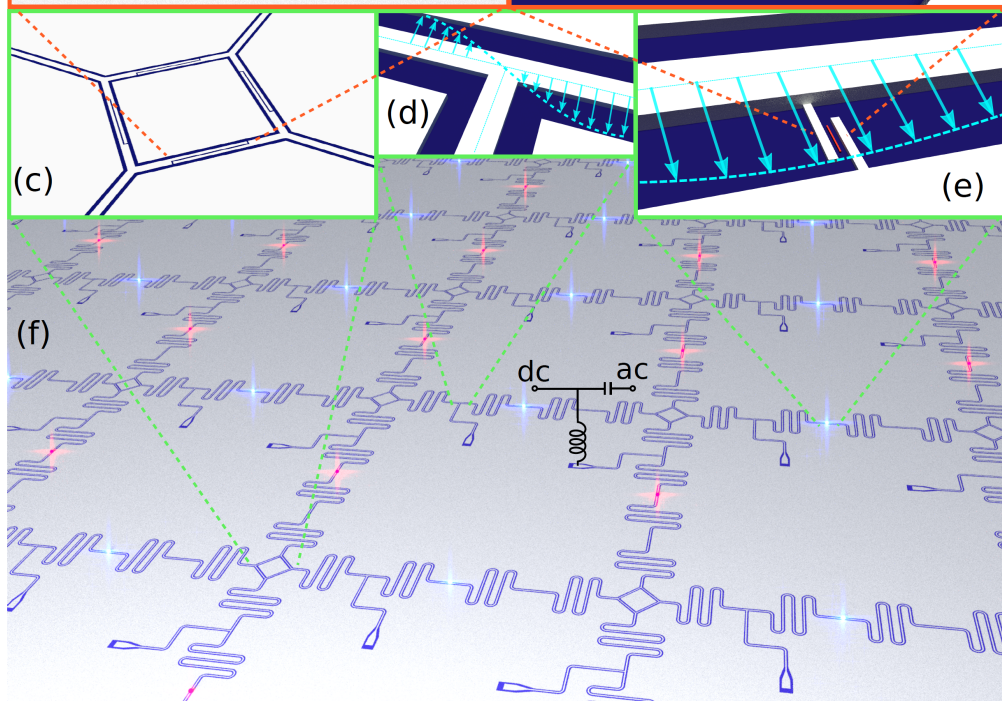
Nigg, Fuhrer, and DL, PRL 118, 147701 (2017)



$$\frac{H}{\hbar} = \sum_{n=1}^N \sum_{m=1}^M \left( \frac{\omega_z}{2} \sigma_{nm}^z + \omega_r a_{nm}^\dagger a_{nm} + \nu_{nm} (a_{nm} \sigma_{nm}^+ + \text{H.c.}) \right) \\ + J \sum_{n,m} (a_{nm}^\dagger a_{nm+1} + a_{nm}^\dagger a_{nm-1} + a_{nm}^\dagger a_{n+1m} + a_{nm}^\dagger a_{n-1m}).$$



hole spin qubit in Ge/Si nanowire



$$\frac{H_{XY}}{\hbar} = \sum_{nm,n'm'} K_{nm,n'm'} \sigma_{nm}^+ \sigma_{n'm'}^- + \text{H.c.},$$

$$K_{nm,n'm'} = \frac{(\Delta m + \Delta n)!}{\Delta n! \Delta m!} \frac{\nu_{nm} \nu_{n'm'}}{\Delta} \left( \frac{J}{\Delta} \right)^{\Delta m + \Delta n}$$

Nigg, Fuhrer, and DL,  
PRL 118, 147701 (2017)

# Parallel syndrome mapping

Nigg, Fuhrer, and DL, PRL 118, 147701 (2017)

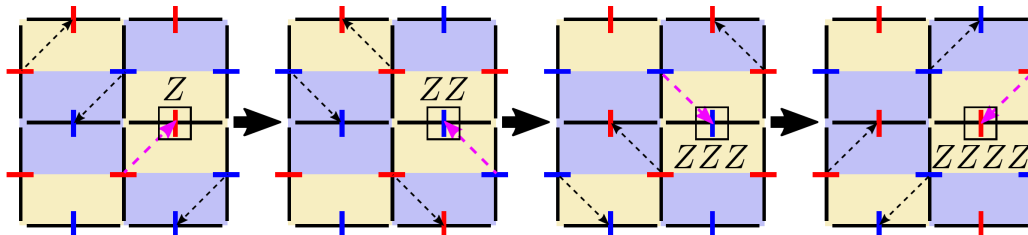


FIG. 2. Frequency layout for parallelization of syndrome mapping in four steps. Red (blue) bars denote qubits at frequency  $\omega_Z^{(r)}$  ( $\omega_Z^{(b)}$ ). The dashed black arrows indicate which couplings are resonant, i.e., active in a given configuration. The mapping of a ZZZZ stabilizer is highlighted as an example (magenta arrows).

# Summary

- Quantum computing with spin qubits in quantum dots
- Decoherence of spin qubits due spin-phonon effects
- Scaling-up: Surface code with floating gates or cavities

*Prospects for Spin-Based Quantum Computing in Quantum Dots*  
Kloeffel and DL, Annu. Rev. Condens. Matter Phys. 4, 51 (2013)